

Synthesis and evaluation of antiproliferative and mPGES-1 inhibitory activities of novel carvacrol-triazole conjugates

İlker Demirbolat^{1,2}, Necla Kulabaş³, Merve Gürboğa⁴,
 Özlem Bingöl Özakpınar⁴, Gamze Çiftçi⁵, Kemal Yelekçi⁵,
 Jianyang Liu⁶, Per-Johan Jakobsson⁶, Özkan Danış⁷, Ayşe Ogan⁷,
 İlkey Küçükgülzel^{3,*}

¹Bezmalem Center of Education, Practice, and Research in Phytotherapy,
 Bezmalem Vakıf University, İstanbul, Türkiye

²Institute of Health Sciences, Marmara University, Dragos 34865, Kartal, İstanbul, Türkiye

³Department of Pharmaceutical Chemistry, Faculty of Pharmacy, Marmara University,
 Başbüyük 34854, İstanbul, Türkiye

⁴Department of Biochemistry, Faculty of Pharmacy, Marmara University,
 Başbüyük 34854, İstanbul, Türkiye

⁵Department of Bioinformatics and Genetics, Faculty of Engineering and Natural Sciences,
 Kadir Has University, İstanbul, Türkiye

⁶Rheumatology Division, Department of Medicine, Solna, Karolinska Institutet & Karolinska University
 Hospital, SE-171 76, Stockholm, Sweden

⁷Department of Chemistry, Faculty of Science, Marmara University, 34722, İstanbul, Türkiye

(Received December 5, 2022; Revised December 28, 2022; Accepted December 29, 2022)

Abstract: Some novel triazole-bearing acetamide derivatives **9-26** were synthesized starting from carvacrol. All synthesized compounds were characterized by FTIR, ¹H-NMR, ¹³C-NMR and MS data. *In vitro* cytotoxic activities of all synthesized molecules against five cancer lines (human breast cancer MCF-7, human lung cancer A549, human prostate cancer PC-3, human chronic myelogenous leukemia K562, human neuroblastoma SH-SY5Y cell lines) were evaluated by MTT assay. Compounds were also tested on mouse embryonic fibroblast cells (NIH/3T3) to determine selectivity. Eighteen target compounds **9-26** were screened for their mPGES-1 and COX-1/2 inhibitory activities. Of these compounds, **26** (KUC16D425) showed the highest mPGES-1 inhibition at 10 µM. This compound has also been observed to induce apoptosis and inhibit cell migration in MCF-7 cells. *In silico* molecular docking calculations were performed to understand the binding interactions of compounds with target proteins. ADMET predictions were also done to evaluate drug-like properties of the novel compounds.

Keywords: Carvacrol; 1,2,4-triazoles; cancer; apoptosis; mPGES-1; *in silico* studies. ©2022 ACG Publication. All rights reserved.

1. Introduction

Cancer, which is characterized by uncontrolled cell division that disrupts normal cell functions, continues to be an important health problem as the second leading cause of death after cardiovascular problems¹. A number of different processes contribute to the development of cancer, including the production of genetic instability, aberrant gene expression, faulty signal transduction, angiogenesis, metastasis, and immune evasion². During the past three decades, cancer mortality has decreased but this group of diseases have still a high death rate, which highlights the ineffectiveness of current treatments such as radiation, chemotherapy, and surgery³. The unwanted side effects of the drugs used in the treatment and the decrease in the quality of life sometimes lead to more problems. Accordingly, the

* Corresponding author: E-mail: ilkay@kucukguzel.com, ikucukguzel@marmara.edu.tr, URL: <http://www.kucukguzel.com>

The article was published by ACG Publications

<http://www.acgpubs.org/journal/organic-communications> © October-December 2022 EISSN:1307-6175

DOI: <http://doi.org/10.25135/acg.oc.142.2212.2651>

Available online: December 30, 2022

primary emphasis of scientists around the world is the discovery of new anticancer drugs. Over the past few decades, research has concentrated on chemically synthesized or naturally derived molecules that act as anticancer agents. Therefore, the discovery of anticancer agents with better tolerable side effects has become an important medical need^{4,5}.

Most of the cancer types are reported to be related to prolonged infection or inflammation⁶. Among all eicosanoids, prostaglandin E₂ (PGE₂), is a potent endogenous lipid associated with inflammation and cancer. It can be produced in many tissues. PGE₂ produced by the enzymes cyclooxygenase-2 (COX-2) and microsomal prostaglandin E synthase 1 (mPGES-1) is pathogenic⁷. Many types of cancer, such as; colon⁸, lung⁹, breast¹⁰, prostate¹¹, gastric adenocarcinoma¹², and neuroblastoma¹³ have been reported to be associated with the enzymes COX-2¹¹ and mPGES-1. Therefore these two enzymes have become crucial as novel targets in the therapy of cancer. Additionally, it is widely recognized that mPGES-1 is connected to the induction of tumor progression^{12,14} and proliferation and angiogenesis are reduced by genetic deletion of mPGES-1¹⁵. It was discovered that MK-886, a FLAP inhibitor that also inhibits mPGES-1, also causes apoptosis through activation of caspase-3¹⁶.

Several types of cancer induce the COX/mPGES-1/PGE₂ pathway, and increased expression of COX-2 and mPGES-1 is associated with decreased survival^{17,18}. A high level of PGE₂ stimulates cancer cell proliferation^{7,19}. The slower tumor growth in mPGES-1-deficient mice^{11,20,21} was associated with reduced angiogenesis¹⁰ and less metastasis¹⁹ and knock-down of mPGES-1 in cancer cells was linked to decreased proliferation in WT mice¹¹.

The two structural isomers of triazole ring system (1,2,3-triazole and 1,2,4-triazole), the isostere of pyrazole, imidazole, oxazole and thiazole moieties, are prominent heterocyclic structures used in designing various bioactive compounds. 1,2,4-Triazoles were formerly reported for their diversified biological activities such as antimicrobial¹⁹, antituberculosis²², analgesic / anti-inflammatory²³ and anticancer⁵. The utilization of 1,2,4-triazole system in pharmaceutical drug design also highlights its importance even in many readily-available commercial medications like ribavirin, fluconazole, itraconazole, voriconazole, alprazolam, estazolam, trapidil, anastrozole, letrozole and rizatriptan.

As shown in Figure 1, examples of 1,2,4-triazole-thioether compounds with previously reported mPGES-1 inhibitory effects are given²⁴⁻²⁶. Compound A, shown in the Figure 1, has a similar structure to the compounds synthesized in this study, and it has been reported to inhibit the mPGES-1 enzyme at a concentration of 9.3 nM²⁴. Rare triazole derivatives (compounds B and C) reported as mPGES-1 inhibitors in the literature have been reported by our group in recently published studies^{25,26}. Among them, compound B, containing carvacrol residue synthesized in the report by Erensoy *et al.* This molecule, which has a triazole-thioether-oxime hybrid structure, became prominent as a lead compound by inhibiting the mPGES-1 enzyme at a submicromolar dose (0.224±0.070 µM)²⁵. Again, according to the results of a study reported by our group in 2016, compound D carrying the triazole-thioether-acetamide hybrid structure obtained from thymol showed remarkable antiproliferative effects in PC3 prostate cancer cells⁵. Knowing that triazole-thioether hybrids made by other research groups also show significant anticancer effects motivated us to continue our work in this area. In some recent papers, anti-cancer activities of several 1,2,4-triazole-ketone (compound E) or acetamide (compound F) hybrids via thioether linkage have been reported and their molecular target was elucidated as VEGFR-2^{27,28}.

A monoterpenic phenol derivative found in the Labiatae family, carvacrol (5-isopropenyl-2-methylphenol) is the starting substance of our study. It can be present in the essential oils of various plants, including wild bergamot (*Citrus aurantium bergamia*), pepperwort (*Lepidium flavum*), oregano (*Origanum vulgare*), thyme (*Thymus vulgaris*), and others²⁹. Antifungal³⁰, antimicrobial³¹, antioxidant³² activities have been reported for carvacrol as well as anticancer³³⁻³⁵ and anti-inflammatory activity^{36,37}. Carvacrol (CV) has high antioxidant activity and has been successfully used, mainly associated with thymol, as dietary phytoadditive to improve animal antioxidant status. The anticancer properties of CV have been reported in preclinical models of breast, liver, and lung carcinomas, acting on proapoptotic processes²⁹. Khan *et al.* report that CV treatment significantly reduced the cell viability of PC-3 cells in a dose- and time-dependent manner and the antiproliferative effect of CV was correlated with apoptosis³⁸. According to Li *et al.*, TRPM7 is found to be expressed and regulate many types of cancers including breast cancer and CV affects breast cancer cells through TRPM7 mediated cell cycle regulation³⁹.

Synthesis and antiproliferative activity of carvacrol-triazole conjugates

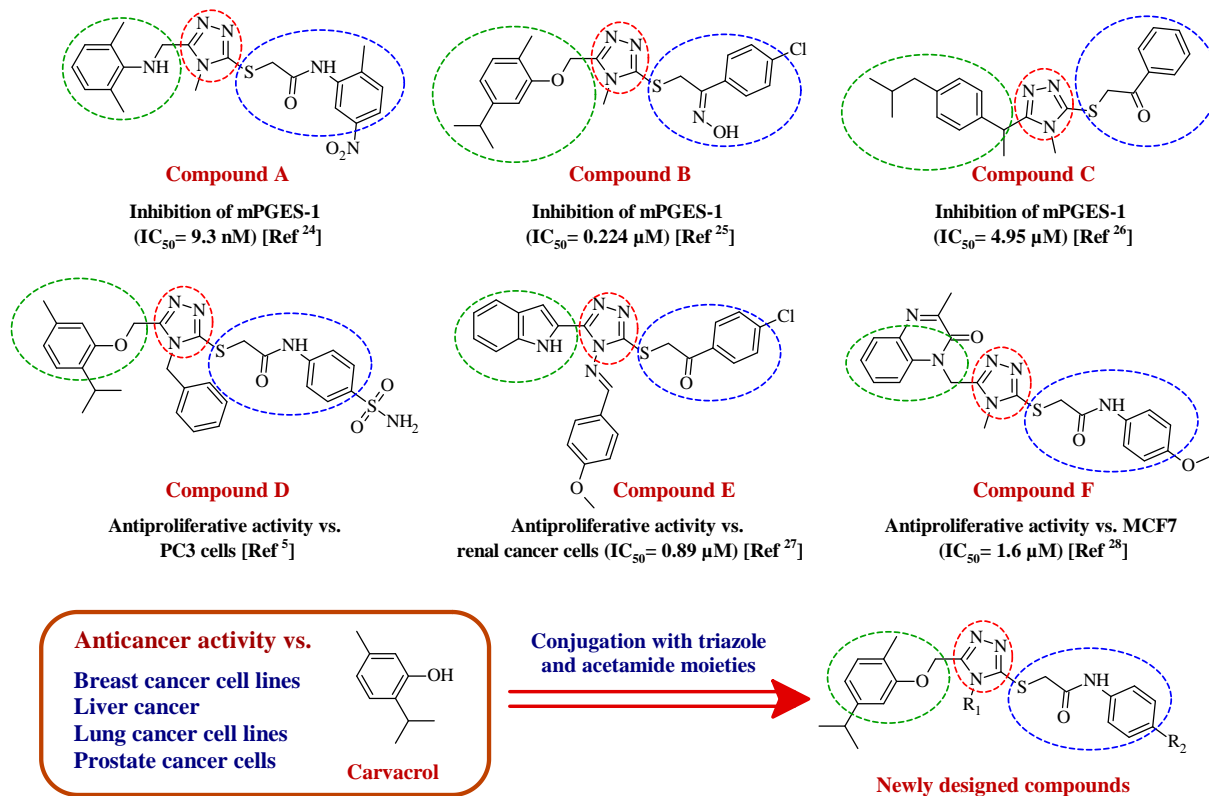


Figure 1. Triazoles reported for antiproliferative and mPGES-1 inhibitory activities and design of novel triazole-acetanilide conjugates from carvacrol

In the light of previous reports on triazolyl sulfanyl acetamides and our previous experiences depicted in Figure 1, we decided to combine carvacrol, 1,2,4-triazole and acetanilide moieties in one molecule in order to target PGE₂ production which is known to lead cancer cell proliferation, migration, resistance to apoptosis and angiogenesis.

2. Experimental

2.1. Chemicals and Instruments

All solvents and reagents were analytical grade and obtained from commercial sources. Melting points were observed in a Thermo IA9300 Basic melting point analyser. Infrared spectra (FTIR) were recorded on a Shimadzu FTIR 8400s and the data is expressed in wavenumbers (cm^{-1}). NMR spectra were recorded on a Bruker Avance NMR spectrometer at 500 MHz for ¹H NMR and 125 MHz for ¹³C NMR. The chemical shifts were expressed in ppm (parts per million) downfield from tetramethylsilane (TMS) using DMSO-*d*₆ as solvent. A Shimadzu Prominence-i LC-2030C 3D Plus high-pressure liquid chromatography system was utilised for purity control. The separations were performed with a GL Sciences Inertsil ODS-3 (4.6×100 mm, 5 μ m) column at 40°C. All experiments were performed in isocratic mode. The mobile phase was consisted of acetonitrile and 0.1% H₃PO₄ in water (70:30, v/v). Flow rate was set to 1 mL/min and the chromatograms were recorded at 254 nm. Elemental analyses were performed with a Leco CHNS 932. A Shimadzu LC-MS/MS-8030 was employed for recording the masses of the synthesised compounds.

2.2. Chemistry

Synthesis of compounds **I-VI**^{40,41} and **1-8**⁵ were performed according to previously described methods. The structure of compounds *N*-phenyl-2-[2-methyl-5-(propan-2-yl)phenoxy]acetyl]hydrazinecarbothioamide **5** and 4-phenyl-5-{[2-methyl-5-(propan-2-yl)phenoxy]methyl}-2,4-dihydro-3*H*-1,2,4-triazole-3-thione **8** were first identified in this study.

2.2.1. Synthesis of compounds 3-5

A mixture of compound **2** (0.05 mol) and ethyl/methyl/phenyl isothiocyanate (0.05 mol) in ethanol (40 mL) was heated under reflux for 4 hours. After completion of the reaction, the solution was cooled to give the crude product, which was filtered and recrystallized from ethanol.

N-Methyl-2-[2-methyl-5-(propan-2-yl)phenoxy]acetyl]hydrazinecarbothioamide (**3**): White solid. Melting point: 179-181 °C²⁵, yield 70%.

N-Ethyl-2-[2-methyl-5-(propan-2-yl)phenoxy]acetyl]hydrazinecarbothioamid (**4**): White solid. Melting point: 138-140 °C²⁵, yield 57%.

N-Phenyl-2-[2-methyl-5-(propan-2-yl)phenoxy]acetyl]hydrazinecarbothioamide (**5**): White solid. Melting point: 170.8-171.6 °C, yield 68%. IR $\bar{\nu}$ (cm⁻¹): 3293, 3219 and 3185 (N-H str), 1672 (C=O), 1534 (N-H bnd), 1252 (C=S). ¹H NMR (300 MHz, DMSO-d₆) /TMS: δ 1.18 (d, 6H, *J*=6.9 Hz, -CH(CH₃)₂); 2.20 (s, 3H, Ar-CH₃); 2.78-2.87 (m, 1H, -CH(CH₃)₂), 4.66 (s, 2H, -O-CH₂-); 6.74-6.77 (m, 2H, Ar-H); 7.06 (d, 1H, *J*=6.9 Hz, Ar-H); 7.17 (t, 1H, *J*=7.2 Hz, Ar-H); 7.32-7.45 (m, 4H, Ar-H); 9.66 (s, 1H, CS-NH-C₆H₅); 9.74 (s, 1H, CONH-NH); 10.13 (s, 1H, -CONH-NH). Anal. Calcd. for C₁₉H₂₃N₃O₂S: C, 63.84; H, 6.49; N, 11.75; S, 8.97. Found: C, 63.47; H, 6.57; N, 11.76; S, 9.46.

2.2.2. Synthesis of compounds 6-8

Compounds **6-8** obtained by refluxing compounds **3-5** (0.03 mol) in 2N NaOH for 4 h. After neutralization with 10% HCl, the solid product was obtained, filtered, dried and recrystallized from ethanol.

4-Methyl-5-[[2-methyl-5-(propan-2-yl)phenoxy]methyl]-2,4-dihydro-3H-1,2,4-triazole-3-thione (**6**): White solid. HPLC *t*_R (min): 13.2, Melting point: 149-151 °C²⁵, yield 52%.

4-Ethyl-5-[[2-methyl-5-(propan-2-yl)phenoxy]methyl]-2,4-dihydro-3H-1,2,4-triazole-3-thione (**7**): White solid. HPLC *t*_R (min): 18.5, Melting point: 100-101.5 °C²⁵, yield 56%.

4-Phenyl-5-[[2-methyl-5-(propan-2-yl)phenoxy]methyl]-2,4-dihydro-3H-1,2,4-triazole-3-thione (**8**): White solid. HPLC *t*_R (min): 8.29, Melting point: 100-103 °C, TLC R_f: 0.57(S₂), yield 58%. IR $\bar{\nu}$ (cm⁻¹): 3030 (N-H str), 2956, 2868 (C-H str), 1575 (N-H bnd), 1282 (C=S). ¹H NMR (500 MHz, CDCl₃/TMS) δ ppm: 1.18 (d, 6H, *J*=6.9 Hz, -CH(CH₃)₂); 1.9 (s, 3H, Ar-CH₃); 2.79-2.81 (m, 1H, -CH(CH₃)₂); 4.92 (s, 2H, -O-CH₂-); 6.63 (s, 1H, Ar-H); 6.76 (d, 1H, *J*=7.5 Hz, Ar-H); 7.01 (d, 1H, *J*=7.7 Hz, Ar-H), 7.43-7.45 (m, 2H, Ar-H); 7.50-7.56 (m, 3H, Ar-H); 12.15 (s, 1H, triazole NH-). ¹³C NMR (125 MHz, CDCl₃/TMS): δ ppm: 15.63, 24.01, 33.97, 60.04, 110.03, 119.63, 124.33, 127.83, 129.70, 130.21, 130.86, 133.03, 148.27, 148.66, 155.24, 169.50. LR-MS (*m/z*): calculated for (M-H)⁻: 338.48, found: 338.15. Anal. Calcd. for C₁₉H₂₁N₃OS: C, 67.23; H, 6.24; N, 12.38; S, 9.45. Found: C, 66.91; H, 6.51; N, 12.64; S, 9.80.

2.2.3. Synthesis of 2-[(4-Alkyl/aryl-5-[[2-methyl-5-(propan-2-yl)phenoxy]methyl]-4H-1,2,4-triazol-3-yl)sulfanyl]-N-(4-substituted phenyl)acetamides (9-26)

0.001 mol of compound **6-8** were dissolved in 10 mL of DMF and 0.002 mol K₂CO₃ were added. The solutions were stirred for 1 hour at room temperature. After mixing for 1 hour, compounds **I-VI** (dissolved in 3 mL of DMF) were added and mixed 12 hours at room temperature. Then the solutions were poured onto ice. The resulting precipitates were washed with water through a membrane filter. The compounds **9-26** were recrystallized from ethanol²⁵.

2-[(4-Methyl-5-[[2-methyl-5-(propan-2-yl)phenoxy]methyl]-4H-1,2,4-triazol-3-yl)sulfanyl]-N-phenylacetamide (**9**): White solid. HPLC *t*_R (min): 4.15, Melting point: 224.5-224.7 °C, yield 61%. IR $\bar{\nu}$ (cm⁻¹): 3246, 3192 (N-H str), 2990, 2856 (C-H str), 1674 (C=O), 1599 (C=N str), 1178 (C-O-C), 715 (C-S). ¹H NMR (500 MHz, DMSO-d₆/TMS) δ ppm: 1.19 (d, 6H, *J*=5.6 Hz, CH(CH₃)₂); 2.07 (s, 3H, Ar-CH₃); 2.81-2.87 (m, 1H, -CH(CH₃)₂); 3.64 (s, 3H, N-CH₃); 4.14 (s, 2H, -S-CH₂-); 5.29 (s, 2H, -OCH₂); 6.76 (dd, 1H, *J*=0.9 and 1 Hz, *J*=6.1 Hz, Ar-H); 7.04-7.08 (m, 3H, Ar-H); 7.31 (t, 2H, *J*=6 Hz,

Synthesis and antiproliferative activity of carvacrol-triazole conjugates

$J=6.6$ Hz, Ar-H); 7.57 (d, 2H, $J=6$ Hz, Ar-H); 10.33 (s, 1H, -NH-). ^{13}C NMR (125 MHz, DMSO- d_6 /TMS): δ ppm: 15.99, 24.36, 30.96, 33.91, 37.95, 60.56, 110.92, 119.25, 119.59, 123.78, 124.03, 129.24, 130.81, 139.26, 148.06, 151.16, 152.81, 155.98, 166.11. LR-MS (m/z): calculated for (M-H) $^-$: 409.17, found: 409.20. Anal. Calcd. for $\text{C}_{22}\text{H}_{25}\text{N}_5\text{O}_4\text{S}$: C, 64.36; H, 6.38; N, 13.65; S, 7.81. Found: C, 64.72; H, 6.18; N, 13.89; S, 7.73.

N-(4-Chlorophenyl)-2-[(4-methyl-5-[[2-methyl-5-(propan-2-yl)phenoxy]methyl]-4H-1,2,4-triazol-3-yl)sulfanyl]acetamide (**10**): White solid. HPLC t_R (min): 6.48, Melting point: 184.4-185.2 °C, yield 62%. IR $\bar{\nu}$ (cm^{-1}): 3238, 3176 (N-H str), 3022-2886 (C-H str), 1674 (C=O), 1610 (C=N str), 1178 (C-O-C), 644 (C-S). ^1H NMR (500 MHz, DMSO- d_6 /TMS) δ ppm: 1.19 (d, 6H, $J=5.6$ Hz, $\text{CH}(\text{CH}_3)_2$); 2.07 (s, 3H, Ar- CH_3); 2.81-2.86 (m, 1H, - $\text{CH}(\text{CH}_3)_2$); 3.63 (s, 3H, N- CH_3); 4.12 (s, 2H, -S- CH_2 -); 5.28 (s, 2H, - OCH_2); 6.76 (dd, 1H, $J=1$ Hz, $J=6.1$ Hz, Ar-H); 7.03-7.05 (m, 2H, Ar-H); 7.36 (d, 2H, $J=7.1$ Hz, Ar-H); 7.59 (d, 2H, $J=7.1$ Hz, Ar-H); 10.46 (s, 1H, -NH-). ^{13}C NMR (125 MHz, DMSO- d_6 /TMS): δ ppm: 16.01, 24.40, 30.95, 33.89, 37.86, 60.52, 110.92, 119.20, 121.13, 123.74, 127.58, 129.19, 130.81, 138.17, 148.04, 151.04, 152.80, 155.97, 166.31. LR-MS (m/z): calculated for (M-H) $^-$: 443.13, found: 443.20. Anal. Calcd. for $\text{C}_{22}\text{H}_{25}\text{ClN}_4\text{O}_2\text{S}$: C, 59.38; H, 5.66; N, 12.59; S, 7.21. Found: C, 59.09; H, 5.13; N, 12.60; S, 6.91.

N-(4-Fluorophenyl)-2-[(4-methyl-5-[[2-methyl-5-(propan-2-yl)phenoxy]methyl]-4H-1,2,4-triazol-3-yl)sulfanyl]acetamide (**11**): White solid. HPLC t_R (min): 6.48, Melting point: 182.3-182.7 °C, yield 59%. IR $\bar{\nu}$ (cm^{-1}): 3240, 3194 (N-H str), 2951-2860 (C-H str), 1668 (C=O), 1614 (C=N str), 1176 (C-O-C), 686 (C-S). ^1H NMR (500 MHz, DMSO- d_6 /TMS) δ ppm: 1.19 (d, 6H, $J=5.5$ Hz, $\text{CH}(\text{CH}_3)_2$); 2.07 (s, 3H, Ar- CH_3); 2.81-2.85 (m, 1H, - $\text{CH}(\text{CH}_3)_2$); 3.63 (s, 3H, N- CH_3); 4.11 (s, 2H, -S- CH_2 -); 5.28 (s, 2H, - OCH_2); 6.76 (dd, 1H, $J=1$ Hz, $J=5.1$ Hz, Ar-H); 7.04 (d, 2H, $J=6.7$ Hz, Ar-H); 7.13-7.16 (m, 2H, Ar-H); 7.56-7.59 (m, 2H, Ar-H); 10.38 (s, 1H, -NH-). ^{13}C NMR (125 MHz, DMSO- d_6 /TMS): δ ppm: 15.98, 24.39, 30.97, 33.94, 37.79, 60.51, 110.91, 115.77, 115.98 ($J=26$ Hz), 119.22, 121.33, 121.39 ($J=7.5$ Hz), 123.76, 130.95, 135.61, 135.62 ($J=1.25$ Hz), 148.09, 151.12, 152.83, 155.99, 157.65, 159.59 ($J=242.5$ Hz), 166.11. LR-MS (m/z): calculated for (M-H) $^-$: 427.16, found: 427.15. Anal. Calcd. for $\text{C}_{22}\text{H}_{25}\text{FN}_4\text{O}_2\text{S}$: C, 61.66; H, 5.88; N, 13.07; S, 7.48. Found: C, 61.76; H, 5.59; N, 13.15; S, 7.60.

N-(4-Bromophenyl)-2-[(4-methyl-5-[[2-methyl-5-(propan-2-yl)phenoxy]methyl]-4H-1,2,4-triazol-3-yl)sulfanyl]acetamide (**12**): White solid. HPLC t_R (min): 7.59, Melting point: 183.7-184.1 °C, yield 57%. IR $\bar{\nu}$ (cm^{-1}): 3169-3099 (N-H str), 3014-2862 (C-H str), 1674 (C=O), 1607 (C=N str), 1179 (C-O-C), 697 (C-S). ^1H NMR (500 MHz, DMSO- d_6 /TMS) δ ppm: 1.24 (d, 6H, $J=5.5$ Hz, $\text{CH}(\text{CH}_3)_2$); 2.11 (s, 3H, Ar- CH_3); 2.85-2.91 (m, 1H, - $\text{CH}(\text{CH}_3)_2$); 3.67 (s, 3H, N- CH_3); 4.17 (s, 2H, -S- CH_2 -); 5.32 (s, 2H, - OCH_2); 6.76 (dd, 1H, $J=0.9$ and 1 Hz, $J=5.1$ Hz, Ar-H); 7.07-7.10 (m, 2H, Ar-H); 7.53-7.59 (m, 4H, Ar-H); 10.51 (s, 1H, -NH-). ^{13}C NMR (125 MHz, DMSO- d_6 /TMS) δ ppm: 15.99, 24.37, 30.94, 33.91, 37.87, 60.52, 110.92, 115.61, 119.21, 121.46, 123.75, 130.82, 130.82, 138.61, 148.05, 151.04, 152.81, 155.97, 166.35. LR-MS (m/z): calculated for (M-H) $^-$: 487.08, found: 489.10. Anal. Calcd. for $\text{C}_{22}\text{H}_{25}\text{BrN}_4\text{O}_2\text{S}$: C, 53.99; H, 5.15; N, 11.45; S, 6.55. Found: C, 54.12; H, 4.70; N, 11.63; S, 6.38.

2-[(4-Methyl-5-[[2-methyl-5-(propan-2-yl)phenoxy]methyl]-4H-1,2,4-triazol-3-yl)sulfanyl]-*N*-(4-nitrophenyl)acetamide (**13**): White solid. HPLC t_R (min): 5.31, Melting point: 224.5-224.7 °C, yield 59%. IR $\bar{\nu}$ (cm^{-1}): 3198-3140 (N-H str), 2990-2864 (C-H str), 1692 (C=O), 1568 (C=N str), 1169 (C-O-C), 710 (C-S). ^1H NMR (500 MHz, DMSO- d_6 /TMS) δ ppm: 1.18 (d, 6H, $J=5.5$ Hz, $\text{CH}(\text{CH}_3)_2$); 2.07 (s, 3H, Ar- CH_3); 2.79-2.85 (m, 1H, - $\text{CH}(\text{CH}_3)_2$); 3.64 (s, 3H, N- CH_3); 4.20 (s, 2H, -S- CH_2 -); 5.28 (s, 2H, - OCH_2); 6.75 (dd, 1H, $J=0.8$, $J=6$ Hz, Ar-H); 7.03 (d, 2H, $J=7$ Hz, Ar-H); 7.79-7.82 (d, 2H, $J=8.3$ Hz, Ar-H); 8.21-8.24 (d, 2H, $J=8.3$ Hz, Ar-H); 10.94 (s, 1H, -NH-). ^{13}C NMR (125 MHz, DMSO- d_6 /TMS) δ ppm: 15.97, 24.34, 30.94, 33.90, 37.91, 60.47, 110.91, 119.20, 119.32, 123.74, 125.52, 130.79, 142.87, 145.30, 148.02, 150.95, 152.84, 155.95, 167.23. LR-MS (m/z): calculated for (M-H) $^-$: 454.15, found: 454.20. Anal. Calcd. for $\text{C}_{22}\text{H}_{25}\text{BrN}_5\text{O}_4\text{S}$: C, 58.01; H, 5.53; N, 15.37; S, 7.04. Found: C, 58.26; H, 5.01; N, 15.45; S, 6.84.

2-[(4-Methyl-5-[[2-methyl-5-(propan-2-yl)phenoxy]methyl]-4H-1,2,4-triazol-3-yl)sulfanyl]-*N*-(4-sulfamoylphenyl)acetamide (**14**): White solid. HPLC t_R (min): 1.99, Melting point: 208.3-208.9 °C,

yield 57%. IR $\bar{\nu}$ (cm⁻¹): 3338 (N-H str), 2950-2870 (C-H str), 1681 (C=O), 1595 (C=N str), 1178 (C-O-C), 657 (C-S). ¹H NMR (500 MHz, DMSO-d₆/TMS) δ ppm: 1.19 (d, 6H, $J=5.5$ Hz, CH(CH₃)₂); 2.07 (s, 3H, Ar-CH₃); 2.50-2.53 (m, 1H, -CH(CH₃)₂); 3.63 (s, 3H, N-CH₃); 4.16 (s, 2H, -S-CH₂-); 5.28 (s, 2H, -OCH₂); 6.77 (dd, 1H, $J=0.9$ Hz, $J=6$ Hz, Ar-H); 7.03-7.05 (m, 2H, Ar-H); 7.31 (s, 2H, -SO₂NH₂-); 7.71-7.78 (m, 4H, Ar-H); 10.66 (s, 1H, -NH-). ¹³C NMR (125 MHz, DMSO-d₆/TMS) δ ppm: 15.99, 24.35, 30.95, 33.92, 37.89, 60.52, 110.92, 119.15, 119.24, 123.74, 124.24, 130.84, 139.16, 142.09, 148.05, 151.03, 152.83, 155.95, 166.76. LR-MS (m/z): calculated for (M-H)⁻: 488.14, found: 488.15. Anal. Calcd. for C₂₂H₂₇N₅O₄S₂: C, 53.97; H, 5.56; N, 14.30; S, 13.10. Found: C, 53.62; H, 5.57; N, 14.36; S, 13.11.

2-[(4-Ethyl-5-[[2-methyl-5-(propan-2-yl)phenoxy]methyl]-4H-1,2,4-triazol-3-yl)sulfanyl]-N-phenylacetamide (**15**): White solid. HPLC t_R (min): 5.79, Melting point: 201.8-202.6 °C, yield 61%. IR $\bar{\nu}$ (cm⁻¹): 3232, 3188 (N-H str), 3012, 2047 (C-H str), 1674 (C=O), 1599 (C=N str), 1178 (C-O-C), 715 (C-S). ¹H NMR (500 MHz, DMSO-d₆/TMS) δ ppm: 1.19 (d, 6H, $J=5.5$ Hz, CH(CH₃)₂); 1.30 (t, 3H, $J=5.8$ Hz, -N-CH₂CH₃); 2.07 (s, 3H, Ar-CH₃); 2.81-2.87 (m, 1H, -CH(CH₃)₂); 4.08-4.11 (q, 2H, N-CH₂); 4.20 (s, 2H, -S-CH₂-); 5.28 (s, 2H, -OCH₂); 6.76 (dd, 1H, $J=0.9$ and 1 Hz, $J=6.1$ Hz, Ar-H); 7.04-7.08 (m, 3H, Ar-H); 7.31 (t, 2H, $J=6.2$ and 6.4 Hz, Ar-H); 7.57 (d, 2H, $J=6.4$ Hz, Ar-H); 10.34 (s, 1H, -NH-). ¹³C NMR (125 MHz, DMSO-d₆/TMS) δ ppm: 15.63, 16.19, 24.34, 33.95, 37.86, 60.26, 110.76, 119.19, 119.67, 123.44, 124.02, 129.25, 131.01, 139.15, 148.07, 150.63, 152.37, 156.92, 165.97. LR-MS (m/z): calculated for (M-H)⁻: 423.18, found: 423.15. Anal. Calcd. for C₂₃H₂₈N₄O₂S: C, 65.07; H, 6.65; N, 13.20; S, 7.55. Found: C, 66.41; H, 6.41; N, 13.61; S, 7.50.

N-(4-Chlorophenyl)-2-[(4-ethyl-5-[[2-methyl-5-(propan-2-yl)phenoxy]methyl]-4H-1,2,4-triazol-3-yl)sulfanyl]acetamide (**16**): White solid. HPLC t_R (min): 9.01, Melting point: 225.6-225.8 °C, yield 63%. IR $\bar{\nu}$ (cm⁻¹): 3127, 3096 (N-H str), 3033, 2821 (C-H str), 1674 (C=O), 1610 (C=N str), 1178 (C-O-C), 644 (C-S). ¹H NMR (500 MHz, DMSO-d₆/TMS) δ ppm: 1.19 (d, 6H, $J=5.6$ Hz, CH(CH₃)₂); 1.32 (t, 3H, $J=5.7$ Hz, -N-CH₂CH₃); 2.07 (s, 3H, Ar-CH₃); 2.81-2.87 (m, 1H, -CH(CH₃)₂); 4.06-4.10 (q, 2H, $J=5.5$, N-CH₂); 4.20 (s, 2H, -S-CH₂-); 5.27 (s, 2H, -OCH₂); 6.76 (dd, 1H, $J=1$ Hz, $J=6.1$ Hz, Ar-H); 7.04-7.05 (m, 2H, Ar-H); 7.37 (d, 2H, $J=6.9$ Hz, Ar-H); 7.59 (d, 2H, $J=6.9$ Hz, Ar-H); 10.48 (s, 1H, -NH-). ¹³C NMR (125 MHz, DMSO-d₆/TMS) δ ppm: 15.59, 16.17, 24.32, 33.27, 37.79, 60.30, 110.69, 119.10, 121.13, 123.33, 127.59, 129.39, 131.17, 138.22, 148.20, 150.61, 152.48, 156.15, 166.27. LR-MS (m/z): calculated for (M-H)⁻: 457.14, found: 457.20. Anal. Calcd. for C₂₃H₂₇ClN₄O₂S: C, 60.18; H, 5.93; N, 12.21; S, 6.99. Found: C, 60.67; H, 5.14; N, 12.39; S, 6.62.

2-[(4-Ethyl-5-[[2-methyl-5-(propan-2-yl)phenoxy]methyl]-4H-1,2,4-triazol-3-yl)sulfanyl]-N-(4-fluorophenyl)acetamide (**17**): White solid. HPLC t_R (min): 5.91, Melting point: 216.2-217.2 °C, yield 56%. IR $\bar{\nu}$ (cm⁻¹): 3194, 3142 (N-H str), 2971, 2842 (C-H str), 1668 (C=O), 1614 (C=N str), 1176 (C-O-C), 686 (C-S). ¹H NMR (500 MHz, DMSO-d₆/TMS) δ ppm: 1.19 (d, 6H, $J=5.5$ Hz, CH(CH₃)₂); 1.32 (t, 3H, $J=5.7$ Hz, -N-CH₂CH₃); 2.07 (s, 3H, Ar-CH₃); 2.81-2.87 (m, 1H, -CH(CH₃)₂); 4.06-4.10 (q, 2H, $J=5.5$, N-CH₂); 4.19 (s, 2H, -S-CH₂-); 5.28 (s, 2H, -OCH₂); 6.76 (d, 1H, $J=6.0$ Hz, Ar-H); 7.05 (d, 2H, $J=4.2$ Hz, Ar-H); 7.37 (t, 2H, $J=7$ Hz, Ar-H); 7.59 (d, 2H, $J=4$ Hz, Ar-H); 10.40 (s, 1H, -NH-). ¹³C NMR (125 MHz, DMSO-d₆/TMS) δ ppm: 15.62, 16.21, 24.34, 33.89, 37.76, 60.22, 110.72, 115.78, 115.98 ($J=25$ Hz), 119.15, 121.33, 121.39 ($J=7.5$ Hz), 123.53, 130.90, 135.66, 148.10, 150.54, 152.22, 156.05, 157.66, 159.58 ($J=240$ Hz), 166.00. LR-MS (m/z): calculated for (M-H)⁻: 441.17, found: 441.20. Anal. Calcd. for C₂₃H₂₇FN₄O₂S: C, 62.42; H, 6.15; N, 12.66; S, 7.25. Found: C, 62.58; H, 6.81; N, 12.80; S, 7.16.

N-(4-Bromophenyl)-2-[(4-ethyl-5-[[2-methyl-5-(propan-2-yl)phenoxy]methyl]-4H-1,2,4-triazol-3-yl)sulfanyl]acetamide (**18**): White solid. HPLC t_R (min): 10.73, Melting point: 224.4-224.7 °C, yield 52%. IR $\bar{\nu}$ (cm⁻¹): 3173, 3099 (N-H str), 2959, 2868 (C-H str), 1672 (C=O), 1607 (C=N str), 1179 (C-O-C), 710 (C-S). ¹H NMR (500 MHz, DMSO-d₆/TMS) δ ppm: 1.19 (d, 6H, $J=5.5$ Hz, CH(CH₃)₂); 1.32 (t, 3H, $J=5.7$ Hz, -N-CH₂CH₃); 2.07 (s, 3H, Ar-CH₃); 2.81-2.87 (m, 1H, -CH(CH₃)₂); 4.06-4.10 (q, 2H, $J=5.6$ Hz, N-CH₂); 4.20 (s, 2H, -S-CH₂-); 5.28 (s, 2H, -OCH₂); 6.76 (d, 1H, $J=6$ Hz, Ar-H); 7.04 (d, 2H, $J=3.3$ Hz, Ar-H); 7.48-7.55 (m, 4H, Ar-H); 10.48 (s, 1H, -NH-). ¹³C NMR (125 MHz, DMSO-d₆/TMS) δ ppm: 15.64, 16.19, 24.11, 33.78, 37.81, 60.11, 110.63, 115.88, 119.16, 121.45, 123.41,

Synthesis and antiproliferative activity of carvacrol-triazole conjugates

130.91, 132.09, 138.75, 148.20, 150.63, 152.33, 156.13, 166.27. LR-MS (m/z): calculated for (M-H)⁻: 501.09, found: 503.20. Anal. Calcd. for C₂₃H₂₇BrN₄O₂S: C, 54.87; H, 5.41; N, 11.13; S, 6.37. Found: C, 54.59; H, 5.67; N, 11.40; S, 6.23.

2-[(4-Ethyl-5-[[2-methyl-5-(propan-2-yl)phenoxy]methyl]-4H-1,2,4-triazol-3-yl)sulfanyl]-N-(4-nitrophenyl)acetamide (**19**): White solid. HPLC t_R (min): 6.84, Melting point: 200.6-201.3 °C, yield 53%. IR $\bar{\nu}$ (cm⁻¹): 3207, 3155 (N-H str), 3001, 2922 (C-H str), 1703 (C=O), 1616 (C=N str), 1171 (C-O-C), 696 (C-S). ¹H NMR (500 MHz, DMSO-d₆/TMS) δ ppm: 1.19 (d, 6H, $J=5.5$ Hz, CH(CH₃)₂); 1.32 (t, 3H, $J=5.7$ Hz, -N-CH₂CH₃); 2.07 (s, 3H, Ar-CH₃); 2.80-2.85 (m, 1H, -CH(CH₃)₂); 4.07-4.11 (q, 2H, $J=5.7$ Hz, N-CH₂); 4.28 (s, 2H, -S-CH₂-); 5.28 (s, 2H, -OCH₂); 6.75 (d, 1H, $J=6.1$ Hz, Ar-H); 7.04 (d, 2H, $J=5.5$ Hz, Ar-H); 7.82 (d, 2H, $J=7.4$ Hz, Ar-H); 8.23 (d, 2H, $J=7.4$ Hz, Ar-H); 10.96 (s, 1H, -NH-). ¹³C NMR (125 MHz, DMSO-d₆/TMS) δ ppm: 15.58, 16.15, 24.36, 33.84, 37.72, 60.17, 110.66, 119.12, 119.32, 123.56, 125.55, 130.88, 142.74, 145.38, 148.15, 150.52, 152.21, 155.83, 166.94. LR-MS (m/z): calculated for (M-H)⁻: 468.17, found: 468.20. Anal. Calcd. for C₂₃H₂₇N₅O₄S: C, 58.83; H, 5.80; N, 14.91; S, 6.83. Found: C, 58.12; H, 5.62; N, 14.98; S, 6.91.

2-[(4-Ethyl-5-[[2-methyl-5-(propan-2-yl)phenoxy]methyl]-4H-1,2,4-triazol-3-yl)sulfanyl]-N-(4-sulfamoylphenyl)acetamide (**20**): White solid. HPLC t_R (min): 2.48, Melting point: 210.9-211.6 °C, yield 52%. IR $\bar{\nu}$ (cm⁻¹): 3250, 3176 (N-H str), 2987-2831 (C-H str), 1668 (C=O), 1608 (C=N str), 1178 (C-O-C), 668 (C-S). ¹H NMR (500 MHz, DMSO-d₆/TMS) δ ppm: 1.19 (d, 6H, $J=5.5$ Hz, CH(CH₃)₂); 1.32 (t, 3H, $J=5.8$ Hz, -N-CH₂CH₃); 2.07 (s, 3H, Ar-CH₃); 2.81-2.87 (m, 1H, -CH(CH₃)₂); 4.07-4.11 (q, 2H, $J=5.7$ Hz, N-CH₂); 4.24 (s, 2H, -S-CH₂-); 5.28 (s, 2H, -OCH₂); 6.76 (dd, 1H, $J=0.9$, $J=5.2$ Hz, Ar-H); 7.04 (m, 2H, Ar-H); 7.27 (s, 2H, -SO₂NH₂-); 7.71-7.78 (m, 4H, Ar-H); 10.68 (s, 1H, -NH-). ¹³C NMR (125 MHz, DMSO-d₆/TMS) δ ppm: 15.63, 16.16, 24.30, 33.89, 37.66, 60.22, 110.65, 119.14, 123.51, 127.29, 130.97, 139.13, 142.07, 148.10, 150.63, 152.21, 156.07, 166.67. LR-MS (m/z): calculated for (M-H)⁻: 502.15, found: 502.20. Anal. Calcd. for C₂₃H₂₉N₅O₄S₂: C, 54.85; H, 5.80; N, 13.91; S, 12.73. Found: C, 54.60; H, 5.64; N, 14.07; S, 12.78.

2-[(5-[[2-Methyl-5-(propan-2-yl)phenoxy]methyl]-4-phenyl-4H-1,2,4-triazol-3-yl)sulfanyl]-N-phenylacetamide (**21**): White solid. HPLC t_R (min): 8.74, Melting point: 167.6-167.9 °C, yield 54%. IR $\bar{\nu}$ (cm⁻¹): 3190, 3117 (N-H str), 2933, 2852 (C-H str), 1666 (C=O), 1600 (C=N str), 1180 (C-O-C), 690 (C-S). ¹H NMR (500 MHz, DMSO-d₆/TMS) δ ppm: 1.14 (d, 6H, $J=5.5$ Hz, CH(CH₃)₂); 1.80 (s, 3H, Ar-CH₃); 2.73-2.79 (m, 1H, -CH(CH₃)₂); 4.20 (s, 2H, -S-CH₂-); 5.13 (s, 2H, -OCH₂); 6.76 (d, 1H, $J=6$ Hz, Ar-H₂₁); 6.82 (s, 1H, Ar-H); 6.94 (d, 1H, $J=6$ Hz, Ar-H); 7.06 (t, 1H, $J=5.8$ Hz, Ar-H); 7.31 (t, 2H, $J=5.9$ Hz, Ar-H); 7.51-7.57 (m, 7H, Ar-H); 10.35 (s, 1H, -NH-). ¹³C NMR (125 MHz, DMSO-d₆/TMS) δ ppm: 15.73, 24.40, 33.84, 37.34, 60.20, 110.66, 119.15, 119.63, 123.72, 124.00, 127.39, 129.28, 130.28, 130.55, 130.71, 133.24, 139.23, 147.86, 152.07, 152.44, 155.77, 166.67. LR-MS (m/z): calculated for (M-H)⁻: 471.18, found: 471.25. Anal. Calcd. for C₂₇H₂₈N₄O₂S: C, 68.62; H, 5.97; N, 11.85; S, 6.78. Found: C, 68.27; H, 5.35; N, 11.90; S, 6.19.

N-(4-Chlorophenyl)-2-[(5-[[2-methyl-5-(propan-2-yl)phenoxy]methyl]-4-phenyl-4H-1,2,4-triazol-3-yl)sulfanyl]acetamide (**22**): White solid. HPLC t_R (min): 13.79, Melting point: 212.5-213.3 °C, yield 55%. IR $\bar{\nu}$ (cm⁻¹): 3178, 3103 (N-H str), 2987, 2843 (C-H str), 1664 (C=O), 1606 (C=N str), 1178 (C-O-C), 690 (C-S). ¹H NMR (500 MHz, DMSO-d₆/TMS) δ ppm: 1.14 (d, 6H, $J=5.5$ Hz, CH(CH₃)₂); 1.79 (s, 3H, Ar-CH₃); 2.74-2.79 (m, 1H, -CH(CH₃)₂); 4.19 (s, 2H, -S-CH₂-); 5.13 (s, 2H, -OCH₂); 6.69 (dd, 1H, $J=1$ Hz, $J=5$ Hz, Ar-H); 6.82 (sd, 1H, $J=1$ Hz, Ar-H); 6.94 (d, 1H, $J=6.2$ Hz, Ar-H); 7.36-7.39 (m, 2H, Ar-H); 7.50-7.61 (m, 7H, Ar-H); 10.49 (s, 1H, -NH-). ¹³C NMR (125 MHz, DMSO-d₆/TMS) δ ppm: 15.64, 24.29, 33.77, 37.24, 60.27, 110.68, 119.15, 121.09, 123.72, 127.33, 127.55, 129.22, 130.30, 130.57, 130.73, 133.22, 138.12, 147.80, 152.06, 152.52, 155.61, 166.06. LR-MS (m/z): calculated for (M-H)⁻: 505.14, found: 505.14. Anal. Calcd. for C₂₇H₂₇ClN₄O₂S: C, 63.96; H, 5.37; N, 11.05; S, 6.32. Found: C, 64.41; H, 5.04; N, 11.25; S, 6.10.

N-(4-Fluorophenyl)-2-[(5-[[2-methyl-5-(propan-2-yl)phenoxy]methyl]-4-phenyl-4H-1,2,4-triazol-3-yl)sulfanyl]acetamide (**23**): White solid. HPLC t_R (min): 9.27, Melting point: 197.7-198.2 °C, yield 52%. IR $\bar{\nu}$ (cm⁻¹): 3240, 3200 (N-H str), 3027, 2864 (C-H str), 1666 (C=O), 1614 (C=N str), 1174 (C-

O-C), 692 (C-S). ^1H NMR (500 MHz, DMSO- d_6 /TMS) δ ppm: 1.14 (d, 6H, $J=5.5$ Hz, $\text{CH}(\text{CH}_3)_2$); 1.79 (s, 3H, Ar- CH_3); 2.74-2.79 (m, 1H, $-\text{CH}(\text{CH}_3)_2$); 4.18 (s, 2H, $-\text{S}-\text{CH}_2-$); 5.13 (s, 2H, $-\text{OCH}_2$); 6.69 (dd, 1H, $J=0.8$ Hz, $J=5.2$ Hz, Ar-H); 6.82 (sd, 1H, $J=0.7$ Hz, Ar-H); 6.94 (d, 1H, $J=6.1$ Hz, Ar-H); 7.14-7.18 (m, 2H, Ar-H); 7.50-7.60 (m, 7H, Ar-H); 10.41 (s, 1H, $-\text{NH}-$). ^{13}C NMR (125 MHz, DMSO- d_6 /TMS) δ ppm: 15.72, 24.29, 33.79, 37.15, 60.27, 110.68, 115.77-115.94 ($J=21$ Hz), 119.15, 121.36, 123.67, 127.34, 130.27, 130.53, 130.71, 133.23, 135.64-135.66 ($J=2.5$ Hz), 147.90, 152.03, 152.52, 155.61, 155.69-159.50 ($J=476$ Hz), 165.78. LR-MS (m/z): calculated for (M-H) $^-$: 489.17, found: 489.20. Anal. Calcd. for $\text{C}_{27}\text{H}_{27}\text{FN}_4\text{O}_2\text{S}$: C, 66.10; H, 5.55; N, 11.42; S, 6.54. Found: C, 65.65; H, 5.45; N, 11.56; S, 6.34.

N-(4-Bromophenyl)-2-[(5-[[2-methyl-5-(propan-2-yl)phenoxy]methyl]-4-phenyl-4H-1,2,4-triazol-3-yl)sulfanyl]acetamide (**24**): White solid. HPLC t_R (min): 16.56, Melting point: 218.9-219.2 °C, yield 49%. IR $\bar{\nu}$ (cm^{-1}): 3176, 3101 (N-H str), 3040, 2864 (C-H str), 1663 (C=O), 1601 (C=N str), 1179 (C-O-C), 698 (C-S). ^1H NMR (500 MHz, DMSO- d_6 /TMS) δ ppm: 1.14 (d, 6H, $J=5.5$ Hz, $\text{CH}(\text{CH}_3)_2$); 1.79 (s, 3H, Ar- CH_3); 2.74-2.79 (m, 1H, $-\text{CH}(\text{CH}_3)_2$); 4.19 (s, 2H, $-\text{S}-\text{CH}_2-$); 5.13 (s, 2H, $-\text{OCH}_2$); 6.69 (dd, 1H, $J=1$ Hz, $J=5.1$ Hz, Ar-H); 6.82 (sd, 1H, $J=0.9$ Hz, Ar-H); 6.94 (d, 1H, $J=6.2$ Hz, Ar-H); 7.49-7.58 (m, 9H, Ar-H); 10.49 (s, 1H, $-\text{NH}-$). ^{13}C NMR (125 MHz, DMSO- d_6 /TMS) δ ppm: 15.74, 24.32, 33.84, 37.34, 60.35, 110.67, 115.57, 119.13, 121.49, 123.69, 127.34, 130.26, 130.55, 130.71, 133.13, 133.22, 138.60, 147.92, 151.97, 152.42, 155.65, 166.12. LR-MS (m/z): calculated for (M-H) $^-$: 549.09, found: 551.10. Anal. Calcd. for $\text{C}_{27}\text{H}_{27}\text{BrN}_4\text{O}_2\text{S}$: C, 58.80; H, 4.93, N, 10.16; S, 5.81. Found: C, 58.41; H, 4.60; N, 10.22; S, 5.45.

2-[(5-[[2-Methyl-5-(propan-2-yl)phenoxy]methyl]-4-phenyl-4H-1,2,4-triazol-3-yl)sulfanyl]-*N*-(4-nitrophenyl)acetamide (**25**): White solid. HPLC t_R (min): 11.07, Melting point: 181.2-181.4 °C, yield 51%. IR $\bar{\nu}$ (cm^{-1}): 3248, 3203 (N-H str), 3036, 2910 (C-H str), 1680 (C=O), 1597 (C=N str), 1167 (C-O-C), 693 (C-S). ^1H NMR (500 MHz, DMSO- d_6 /TMS) δ ppm: 1.13 (d, 6H, $J=5.5$ Hz, $\text{CH}(\text{CH}_3)_2$); 1.78 (s, 3H, Ar- CH_3); 2.73-2.79 (m, 1H, $-\text{CH}(\text{CH}_3)_2$); 4.26 (s, 2H, $-\text{S}-\text{CH}_2-$); 5.13 (s, 2H, $-\text{OCH}_2$); 6.69 (dd, 1H, $J=1$ Hz, $J=5$ Hz, Ar-H); 6.82 (sd, 1H, $J=1$ Hz, Ar-H); 6.94 (d, 1H, $J=6.3$ Hz, Ar-H); 7.50-7.60 (m, 5H, Ar-H); 7.80-7.83 (d, 2H, $J=7.3$ Hz, Ar-H); 8.22-8.25 (d, 2H, $J=7.3$ Hz, Ar-H); 10.96 (s, 1H, $-\text{NH}-$). ^{13}C NMR (125 MHz, DMSO- d_6 /TMS) δ ppm: 15.72, 24.29, 33.77, 37.29, 60.26, 110.68, 119.17, 121.32, 123.68, 125.53, 127.30, 130.31, 130.58, 130.71, 133.19, 142.86, 145.35, 147.87, 151.84, 152.47, 155.71, 167.00. LR-MS (m/z): calculated for (M-H) $^-$: 516.17, found: 516.20. Anal. Calcd. for $\text{C}_{27}\text{H}_{27}\text{N}_5\text{O}_4\text{S}$: C, 62.65; H, 5.26; N, 13.53; S, 6.19. Found: C, 62.03; H, 4.87; N, 13.59; S, 6.20.

2-[(5-[[2-Methyl-5-(propan-2-yl)phenoxy]methyl]-4-phenyl-4H-1,2,4-triazol-3-yl)sulfanyl]-*N*-(4-sulfamoylphenyl)acetamide (**26**): White solid. HPLC t_R (min): 3.44, Melting point: 187.5-188.2 °C, yield 53%. IR $\bar{\nu}$ (cm^{-1}): 3323, 3252 (N-H str), 2958 (C-H str), 1672 (C=O), 1593 (C=N str), 1176 (C-O-C), 657 (C-S). ^1H NMR (500 MHz, DMSO- d_6 /TMS) δ ppm: 11.14 (d, 6H, $J=5.5$ Hz, $\text{CH}(\text{CH}_3)_2$); 1.79 (s, 3H, Ar- CH_3); 2.74-2.79 (m, 1H, $-\text{CH}(\text{CH}_3)_2$); 4.23 (s, 2H, $-\text{S}-\text{CH}_2-$); 5.13 (s, 2H, $-\text{OCH}_2$); 6.69 (dd, 1H, $J=0.7$ Hz, $J=5.3$ Hz, Ar-H); 6.82 (s, 1H, Ar-H); 6.94 (d, 1H, $J=6.1$ Hz, Ar-H); 7.27 (s, 2H, $-\text{SO}_2\text{NH}_2-$); 7.50-7.60 (m, 5H, Ar-H); 7.71-7.79 (m, 4H, Ar-H); 10.69 (s, 1H, $-\text{NH}-$). ^{13}C NMR (125 MHz, DMSO- d_6 /TMS) δ ppm: 15.73, 24.37, 33.78, 37.24, 60.28, 110.69, 119.14, 123.69, 127.24, 127.34, 130.29, 130.57, 130.71, 133.21, 139.13, 142.15, 147.87, 151.94, 152.44, 155.66, 166.54. LR-MS (m/z): calculated for (M-H) $^-$: 550.15, found: 550.15. Anal. Calcd. for $\text{C}_{27}\text{H}_{29}\text{N}_5\text{O}_4\text{S}_2$: C, 58.78; H, 5.30; N, 12.69; S, 11.62. Found: C, 58.32; H, 4.93; N, 12.58; S, 11.19.

2.3. Biological Methods

2.3.1. Cell Culture

Human chronic myelogenous leukemia (K562), human breast cancer (MCF-7), human lung cancer (A549), human prostate cancer (PC-3), human neuroblastoma (SH-SY5Y), and mouse embryonic fibroblast (NIH/3T3) cells were used for cell culture. The cells were grown in Dulbecco's modified Eagle medium (DMEM) from Gibco, Rockville, Maryland, USA, which contains 10% fetal bovine serum (FBS) and are kept in an incubator at 37°C and 5% CO_2 . At 80–90% confluence, cell passage was carried out.

Synthesis and antiproliferative activity of carvacrol-triazole conjugates

2.3.2. Cell Viability Assay

The 3-(4,5-dimethylthiazol-2-yl)-2,5-diphenyltetrazolium bromide (MTT) assay was carried out to evaluate cell viability. In 96-well plates, cells (1×10^4 cells/well) were seeded and incubated overnight. The cells were treated with different concentrations (1–50 μM) of synthesised compounds (**9-26**) for 48 h. MTT was added to each well at a final concentration of 0.5 mg/mL after the initial incubation time and incubated for an additional 4 hours. Following the removal of the growth medium, 100 microliters of SDS buffer were added in order to dissolve the purple formazan product. Using a microplate reader, absorbances at 570 and 630 nm wavelengths were measured (BioTek, Winooski, VT, USA)⁴².

2.3.3. Measurement of Caspase Enzymes Activities

The caspase colorimetric test kits were used to evaluate the activity of caspase-3, caspase-8, and caspase-9. The manufacturer provided assay guidelines (Millipore, USA). After 24 hours, treated (50 and 100 μl) and untreated cells were collected and resuspended in cold, ready-to-use lysis solution for 15 minutes. The supernatants were obtained following high-speed centrifugation and used for analyses of caspase activity. Reaction buffer, DTT, DEVD-p-NA, Ac-IETD-pNA, and Ac-LEHD-pNA substrates for caspase-3, caspase-8, and caspase-9, were added respectively before the samples were incubated at 37°C for 2 hours. According to the theory, the amino acid sequence Asp-Glu-Val-Asp is recognized by caspase-3 made from cellular lysate (DEVD). The assay relies on spectrophotometric detection of the chromophore p-nitroaniline (p-NA) after cleavage from the labelled substrate (DEVD-p-NA). p-NA light emission can be measured at 405 nm with a microtiter plate reader. Caspase-3, caspase-8, and caspase-9 activity can be measured by comparing the absorbance of p-NA from an apoptotic sample with an untreated control sample.

2.3.4. Measurement of Mitochondrial Membrane Potential (MMP)

The decrease in MMP was determined with the JC-1 mitochondrial membrane potential (MMP) kit (MitoPT JC-1, ImmunoChemistry Technologies, LLC). JC-1, a lipophilic cation, is widely used to monitor mitochondria health in apoptosis studies. The membrane-penetrating dye JC-1 reveals potential-dependent accumulation in mitochondria, as indicated by a fluorescence emission shift from green (~529 nm) to red (~590 nm). Depending on the MMP, JC-1 forms J-aggregates associated with a large emission shift (590 nm). As the mitochondrial membranes depolarize, the dyestuff changes reversibly from orange to green. For JC-1 staining, after the incubation of compounds, cell suspensions were adjusted to a density of 0.5×10^6 cells/mL and incubated in assay buffer with JC-1 (10 $\mu\text{g/mL}$) for 15 minutes at 37°C in the dark. The cells were collected by centrifugation at 1000 rpm for 10 minutes. The plate was read at 510 and 585 nm wavelengths by fluorescence Elisa reader. Finally, 585/510 values were calculated to determine the changes in MMP.

2.3.5. Wound-Healing Assay

The influence of compound **26** on motility and migration of MCF-7 cells were investigated by the use of a wound-healing assay²⁶. In order to achieve approximately 90% confluence, cancer cells were seeded in six-well dishes. Using a sterile 200- μL pipette tip, a straight-line scratch mimicking a monolayer wound was created. After the scratch was made, the wells were gently washed with PBS to remove detached cells and a fresh, serum-free medium was added. MCF-7 cells were treated with vehicle as control (untreated cells) and treated with compound **26** at concentrations of 20 μM and 50 μM to see its effect on migration. The plates were then incubated at 37°C and the rate of cell movement across the cavity was observed. Digital recording at the same position was made after scratching at time zero (T₀) and 24 h and stored by a computerized imaging system (Leica DC300F camera). Effects on cell motility and migration were predicted using ImageJ program (National Institutes of Health, Bethesda, MD, USA). The area of the remaining wound was determined as the ratio between the residual area at a given time point and the original wound area (T₀) \times 100.

2.3.6. Preparation of Human mPGES-1 Membrane Fraction and PGES Activity Assay

Human mPGES-1 was cloned into the pSP19T7LT vector and expressed in *E. coli* BL21 cells which harboured the pLysSL plasmid. Cells were then cultured in TB medium containing ampicillin (100 µg/mL) and chloramphenicol (20 µg/mL) at 37 °C with shaking (250 rpm). When OD₆₀₀ reached 0.5, 1 mM IPTG was added to induce mPGES-1 expression and cells were cultured for another 3 hours before harvesting by centrifuging at 3,000 × g for 10 min at 4°C. Cells pellets were lysed by 3 freeze-thawing cycles and DNA was removed by incubation with 10 mM MgCl₂ and 0.4 µg/mL DNase for 30min on ice. The lysate was then sonicated on ice for 6 × 30 s at 60% power. Cell debris were removed by centrifuging at 5,000 × g at 4°C. Membrane fraction was obtained by ultracentrifugation at 230,000 × g for 1 hour at 4°C, and resuspended in 1 mL 20 mM sodium phosphate buffer containing 10% glycerol and 1 mM glutathione. The protein concentration was measured with nanodrop at 280 nm.

2-Thiobarbituric acid (TBA) – malondialdehyde (MDA) assay was performed to examine the inhibitory potential of selected compounds as described before⁴³. Briefly, human membrane fraction (100 µg) produced from *E. coli* was pre-incubated with test compounds on ice for 30 minutes. PGH₂ (final concentration at 25 µM) was then added to the enzyme-compound mixture and incubated for 90 seconds at room temperature. The reaction was quenched by adding acidified FeCl₂, which converts remaining PGH₂ to 12-hydroxyheptadecatrienoic acid (12-HHT) and MDA. Finally, TBA was added and MDA-TBA2 adduct was formed by incubation at 80°C for 30 minutes. Fluorescence was measured at 485 nm (excitation)/535 nm (emission). 1-{6-Chloro-5-methyl-1-[6-(trifluoromethyl)pyridin-2-yl]-1H-benzimidazol-2-yl}-N-(oxolan-3-yl)piperidine-4-carboxamide (compound **118**) which was reported as a potent mPGES-1 inhibitor was used as reference compound⁴³.

2.3.7. In vitro COX-1/2 Enzyme Inhibition Assay

In order to determine their selectivity for mPGES-1 over COX-1/2 (a mixture of equal amount of COX-1 and COX-2), the most promising mPGES-1 inhibitors were assayed for their inhibitory activities on COX-1/2 using an enzyme immunoassay-based ‘COX (ovine/human) Inhibitor Screening Assay’ kit (#560131, Cayman Chemical, Ann Arbor, MI, USA). According to the kit’s manual, 100 µM concentration of all samples were incubated with COX-1/2 for 10 minutes at 37 °C and reaction was started with the addition of 10 µL arachidonic acid (2 mM) as substrate. After incubation at 37 °C for exactly 2 minutes, the enzymatic reaction was terminated by addition of 30 µL saturated stannous chloride in hydrochloric acid to produce prostaglandin F_{2α} (PGF_{2α}) in the presence of prostaglandin H₂ (PGH₂). After the final incubation of the reaction mixture for 5 minutes at room temperature, the resulting PGF_{2α} was assayed by ELISA according to the manufacturer’s instructions using Epoch Absorbance Microplate Reader (BioTek Instruments, Inc., Winooski, VT, USA). All of the assays were carried out in triplicate and the inhibitory activity of the tested compounds were expressed as % inhibition against COX-1/2 enzymes at the concentration of 100 µM.

2.4. In Silico Methods

2.4.1. Molecular Modeling Methods

The structures of compound **26**, reference molecule MK-886¹⁶ and three co-crystallized inhibitors were modeled using the Biovia Discovery Studio 4.5 (DS) (Dassault Systems BIOVIA, 2017) program and optimized with using DS ligand preparation tool. For molecular docking experiments, mPGES-1 (PDB ID: 5K0I, resolution: 1.30 Å)⁴⁴, COX-1 (PDB ID: 5WBE, resolution: 2.75 Å)⁴⁵ and COX-2 (PDB ID: 3NT1, resolution: 1.73 Å)⁴⁶ enzyme structures were downloaded from Protein Data Bank (<https://www.rcsb.org>). These enzymes were cleared off co-crystallized inhibitor, water molecules and non-interacting ions besides the addition of all missing residues and hydrogens. BIOVIA "Prepare Macromolecule" toolkit were used for preparing these enzymes and AutoDock 4.2.6 docking software (<http://autodock.scripps.edu>)⁴⁷ was utilized for all docking calculations. While the grid box of 50 × 50 × 50 Å was chosen, the grid center coordinates of the mPGES-1 enzyme were 9.697, 15.296, 27.28 (x, y, z). The grid center coordinates of the COX-1 enzyme were 37.205, 163.297, 27.409 (x, y, z), and the grid center coordinates of the COX-2 enzyme were set as -54.506, -55.797, -11.193 (x, y, z). The proteins were kept rigid and all ligands were flexible in the docking process. Autodock 4.2's Lamarckian Genetic Algorithm⁴⁸ was used with a 20,000,000 energy rating. Ten independent calculations were

respectively⁵. In the ¹H NMR spectrum, resonances assigned to the N¹-H, N²-H and N⁴-H protons of compound **5** were detected at 10.13, 9.74 and 9.66 ppm, respectively⁵¹.

In the IR spectrum of compound **8**, the disappearance of C=O stretching band of the acylthiosemicarbazides and detecting of C=S stretching band at 1282 cm⁻¹ is an evidence for ring closure form of 1,2,4-triazole-3-thione. Further evidence for 1,2,4-triazole-3-thione ring formation was the lack of a N-H peak of thiosemicarbazide **5** at 9.66-10.13 ppm and the detection of signal at 12.15 ppm, due to the presence of triazole N-H proton⁵¹. ¹³C NMR spectra of compound **8** have signals of triazole thiocarbonyl (C=S) at 169.50 ppm²⁵.

The IR spectra of compounds **9-26** were characterized by the presence of new N-H stretching band, C=O stretching band and C-S-C absorption band at 3157-3030 cm⁻¹, 1703-1663 cm⁻¹ and 715-644 cm⁻¹, respectively. In the ¹H NMR spectra of compound **9-26**, signals at about 4.11-4.28 ppm and 10.33-10.96 ppm that were attributed to the α-thioacetamide group of -CH₂- protons and N-H proton respectively while N-H peak of the 1,2,4-triazol-3-thione disappeared⁵. ¹³C NMR spectra of compounds **9-26** showed the presence of new carbonyl peak (C=O) due to α-thioacetamide group between 165.78-167.23 ppm. Low resolution mass spectra (LR-MS) supported the molecular weights of compounds **9-26**. Furthermore, all new compounds synthesized in the present study gave elemental analysis data consistent to assigned structures⁵.

3.2. Biological Activity Studies

3.2.1. Cytotoxic Activity of the Synthesized Compounds

Compounds **9-26** were investigated for their antiproliferative activity using MCF-7, A549, PC-3, K562, SH-SY5Y and NIH/3T3 cells. MTT assay was used for determination of cytotoxicity. No significant cytotoxic effect was observed in DMSO-treated samples. The compounds were also tested for inhibitory effects in NIH-3T3. The results of the first-line screening data at 10 μM were summarized in Table 1.

Table 1. Cytotoxicity profiles of compounds **9-26** expressed as percentage inhibition of proliferation observed with cancer cell lines

Compound	Lab ID codes	% Inhibition of proliferation					
		MCF7	A549	PC-3	K562	SH-SY5Y	NIH3T3
9	KUC16D094	14.35	4.85	-10.87	-1.95	-4.99	-5.15
10	KUC16D097	41.95	30.96	-4.95	20.72	3.65	-1.14
11	KUC16D103	30.63	18.78	-1.58	10.79	8.76	-5.44
12	KUC16D111	40.62	31.09	-2.19	14.29	1.26	30.26
13	KUC16D112	38.19	32.81	6.38	0.10	13.00	26.75
14	KUC16D115	25.14	9.39	-5.61	-5.54	0.79	4.65
15	KUC16D125	17.52	18.26	-29.13	13.04	-15.99	38.48
16	KUC16D128	23.75	8.61	-21.12	16.82	-14.96	27.11
17	KUC16D134	24.64	13.82	-39.03	12.97	-3.77	21.82
18	KUC16D142	20.83	15.55	-13.42	11.58	-9.39	29.69
19	KUC16D143	41.51	37.19	18.42	15.49	3.34	26.82
20	KUC16D146	23.75	22.12	-1.33	6.93	3.77	11.16
21	KUC16D404	33.70	40.58	-15.05	11.22	-6.00	33.19
22	KUC16D407	37.16	28.90	-16.12	11.27	-6.01	29.54
23	KUC16D413	30.33	8.40	-20.92	11.15	-10.45	23.53
24	KUC16D421	28.70	13.46	-16.63	10.01	-12.33	26.11
25	KUC16D422	27.36	20.29	-17.70	20.59	-7.07	14.80
26	KUC16D425	19.29	11.11	7.40	10.14	7.93	10.51

Since MCF-7 was the cell line in which the synthesized compounds showed the highest inhibition values on average, a further study was performed to determine the IC₅₀ values of compounds

Synthesis and antiproliferative activity of carvacrol-triazole conjugates

9-26 in these cells as demonstrated in Table 2. As a result of this study, IC_{50} values were obtained which surprisingly did not correlate with inhibition values at 10 μM concentration, and compound **26** emerged as the most active 1,2,4-triazole derivative. All remaining compounds were found to be ineffective with IC_{50} values above 100 μM . Compound **26** was found to be more effective than the reference drug doxorubicin on MCF-7 cells with an IC_{50} value of 12.8 μM .

Table 2. Dose-dependent antiproliferative activity of compounds **9-26** on MCF-7 cell lines

Compound	IC_{50} (μM)		Compound	IC_{50} (μM)	
	MCF-7	NIH3T3		MCF-7	NIH3T3
9	>100	>100	18	>100	>100
10	>100	>100	19	>100	>100
11	>100	>100	20	>100	>100
12	>100	>100	21	>100	>100
13	>100	>100	22	>100	>100
14	>100	>100	23	>100	>100
15	>100	>100	24	>100	>100
16	>100	>100	25	>100	>100
17	>100	>100	26	12.8	31.06
			Doxorubicin	49.05	>100

Although compound D (Figure 1) synthesized from thymol as the starting material in our previous study had an IC_{50} value of 5.96 μM against PC-3 cancer cell line, in this study, none of the new compounds synthesized from carvacrol (the structural isomer of thymol) showed any effect against PC-3 cancer cell line⁵. In contrast, significant inhibition was detected for compound **26** against MCF-7 cell line with 12.8 μM IC_{50} value.

3.2.2. Apoptosis Studies

As the most effective molecule was determined as compound **26** as a result of MTT tests and IC_{50} determinations, apoptosis studies were performed on this compound. Biochemical and morphological methods were used to demonstrate the apoptotic effects of compound **26** on MCF-7 cells. Firstly, Annexin V staining was carried out to detect early apoptosis in cells^{52,53}. This procedure is based on phosphatidylserine, which is found in the inner part of healthy cell membranes, and rises to the outer part of the cell in apoptotic cells. Dose-dependent efficacy studies were performed using compound **26** at 10 μM and 50 μM concentrations. Although there was a dose-related increase in the number of early apoptotic cells in Annexin V binding assays, this increase was not statistically significant ($p > 0.05$) (Figure 2).

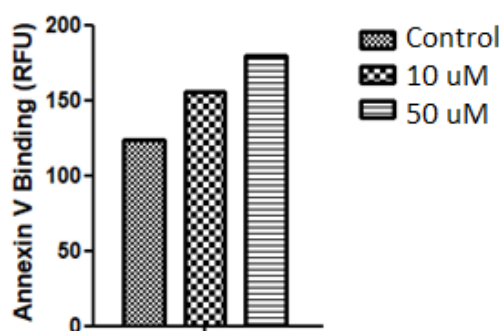


Figure 2. Effect of compound **26** on early apoptosis in breast cancer cells

In apoptotic cell death, there are two processes carried out by the caspases: the extrinsic (mitochondrial) pathway initiated by Caspase-8 and the activation of intrinsic pathways triggered by caspase-9, triggering cell death. The most frequently measured caspase activity at the end of extrinsic or intrinsic apoptotic processes is that of caspase-3⁵²⁻⁵⁴. As a result of assays for caspase enzyme activation, it was determined that compound **26** induced apoptosis in MCF-7 cells (Figure 3). While compound **26** induced apoptosis in a dose-dependent manner, it was found to exert this effect by inducing Caspase-9 signaling, also called the mitochondrial pathway, which was statistically significant ($p < 0.001$).

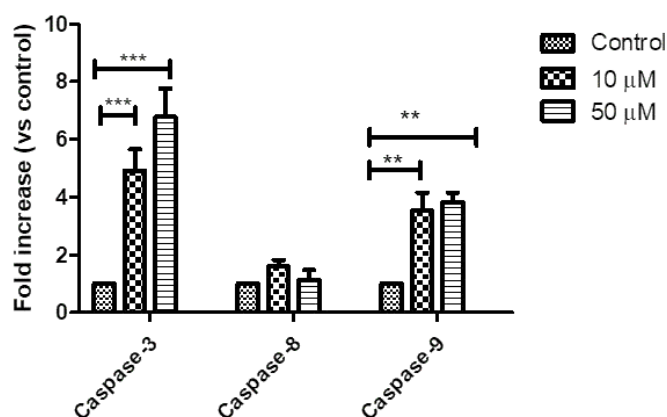


Figure 3. Effects of compound **26** on caspase enzymes activation in MCF-7 cells

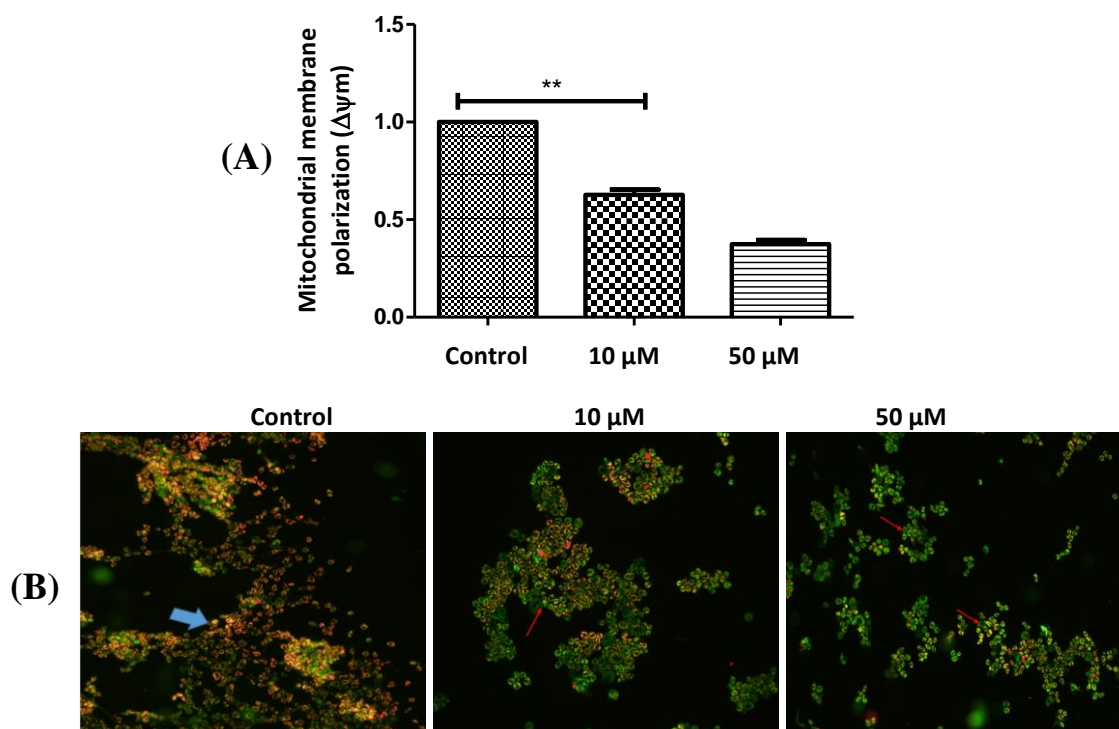


Figure 4. Determination of mitochondrial membrane potential in MCF-7 cells by JC-1 staining. Blue arrow indicates healthy cells whereas red arrows indicate apoptotic cells. A) Membrane depolarization B) Morphological demonstration of mitochondrial membrane depolarization

JC-1 staining was used to confirm the activity of the internal apoptotic pathway. A dye called JC-1 is used to determine mitochondrial membrane polarization. Effects of compound **26** on mitochondrial membrane polarization (MMP) have also been investigated. The JC-1 dye aggregates in

Synthesis and antiproliferative activity of carvacrol-triazole conjugates

mitochondria in healthy cells, giving it a red fluorescent color. In apoptotic cells, on the other hand, since the mitochondrial membrane potential collapses, the JC-1 dye cannot accumulate in the mitochondria and retains its monomeric form in the cytoplasm, giving a green fluorescent color. In our previous study, it was reported that compound D, whose antiproliferative activity was detected, induced apoptotic cell death by triggering the intrinsic pathway and significantly reduced the mitochondrial membrane potential⁵. Similarly, JC-1 staining revealed that the intrinsic pathway, which starts with caspase-9 activation and results in decreased mitochondrial membrane potential, is triggered by compound **26** (Figure 4). This increase was also found to be statistically significant at 50 μM dose ($p < 0.001$). Although it was observed that membrane polarization increased at 10 μM dose, it was not found to be statistically significant ($p > 0.05$).

3.2.3. Effect of Compound **26** on Cell Migration

In order to determine the inhibitory effect of compound **26** on cell migration, a wound-healing assay was utilized. In the wound-healing assay, cell migration was monitored for 0 h and 24 h. As a result of wound-healing experiments, it was determined that the compound **26** inhibited cell migration after 24 h. This inhibition was found to be more prominent, especially at the 10 μM dose (Figure 5).

3.2.4. Inhibition of mPGES-1 and COX-1/2 Enzymes

Compounds **9-26** were screened for their inhibition potential on mPGES-1 enzyme. Compound **118**, which has been reported as a potent mPGES-1 inhibitor by Larsson *et al.*⁴³, was used as reference compound. As seen in Table 3, it was determined that the synthesized compounds had a marginal or no effect on mPGES-1 activity at 10 μM .

Table 3. Inhibition profile of compounds **9-26** against mPGES-1 and COX-1/2

Compound	Lab ID codes	mPGES-1			% Inhibition of COX-1/2 at 100 μM
		% Inhibition	P value	P value (-log ₁₀)	
9	KUC16D094	1.911	0.540	0.268	10.9
10	KUC16D097	5.605	0.159	0.799	10.6
11	KUC16D103	0.983	0.680	0.167	14.9
12	KUC16D111	2.830	0.258	0.588	15.7
13	KUC16D112	1.602	0.352	0.453	14.3
14	KUC16D115	5.158	0.053	1.275	14.3
15	KUC16D125	-0.491	0.937	0.028	14.5
16	KUC16D128	5.787	0.012	1.910	14.4
17	KUC16D134	8.135	0.028	1.555	15.4
18	KUC16D142	4.260	0.466	0.332	8.1
19	KUC16D143	-0.061	0.967	0.015	7.8
20	KUC16D146	8.170	0.111	0.955	N.D. ^a
21	KUC16D404	0.253	0.555	0.256	8.9
22	KUC16D407	1.221	0.487	0.312	0.4
23	KUC16D413	0.709	0.415	0.382	7.9
24	KUC16D421	4.972	0.489	0.311	16.6
25	KUC16D422	0.462	0.837	0.078	10.6
26	KUC16D425	18.951	0.008	2.075	17.9
Compd 118 ^a		73.780	0.000	4.030	
Dexketoprofen					65.3
Ibuprofen					68.1
Celecoxib					N.D. ^b

^a Compound **118**, reported by Larsson *et al.*⁴³, was used as reference compound.

^b Not determined; inhibition at this concentration is below the linear value of the calibration plot (too low inhibition)

^c Not determined; inhibition at this concentration is above the linear value of the calibration plot (too high inhibition)

Among the 18 synthesized molecules, compound **26** with 18.95% enzyme inhibition potential was selected for further studies. The IC_{50} value of this compound was determined to be higher than 100 μM , as evident from the dose-response curve presented in Figure 6. Whereas, in our previous study, the synthesized 2- $\{[3-[1-[5\text{-methyl-2-(propane-2-yl)phenoxy]ethyl]-4\text{-substituted-4,5-dihydro-1,2,4-triazole]sulfanyl}\}-1\text{-(substituted phenyl)ethanone derivatives from carvacrol had showed significant mPGES-1 inhibition (IC_{50} values are between 1.46-3.83)²⁵. Further, the inhibitory activity against COX isozymes was also evaluated for compounds **9-26**. The protein mixture contained equal amounts of COX-1 and COX-2 enzymes. Thus, when a compound can remarkably inhibit either COX-1 or COX-2, it will exhibit the significant inhibitory activity against the mixed COX-1 and COX-2. Similar to the results of our previous study²⁵, as shown in Table 3, none of the new 1,2,4-triazoles derivatives with an amide moiety via thioether linkage showed noteworthy inhibition against COX-1/2, too; therefore, there was no need to determine their IC_{50} values.$

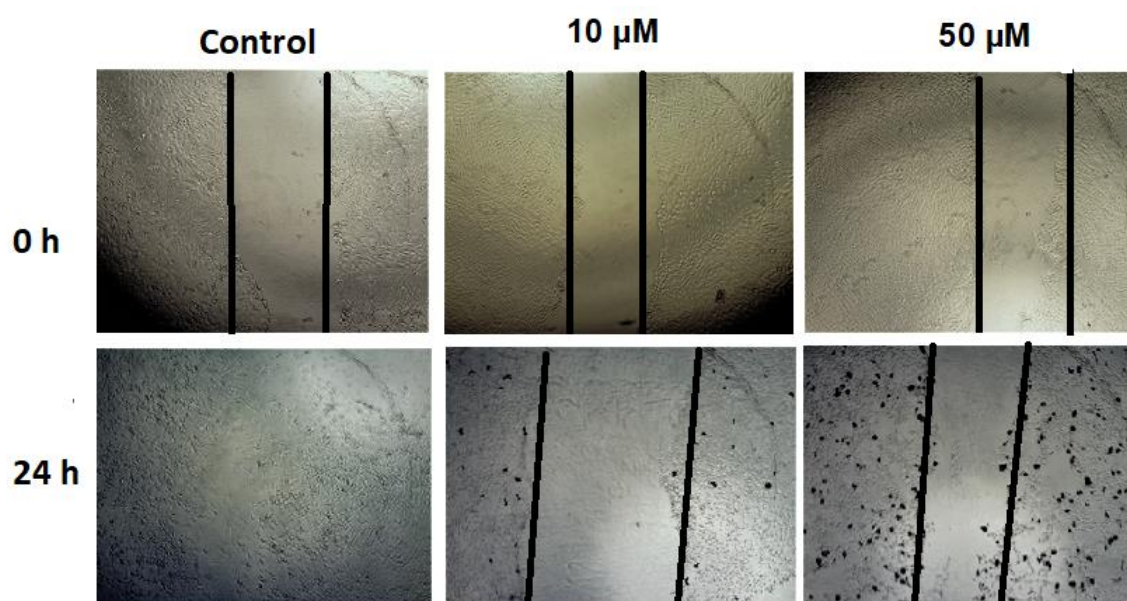


Figure 5. Wound healing assay results showing the potential of compound **26** to inhibit cell migration on MCF7 cells

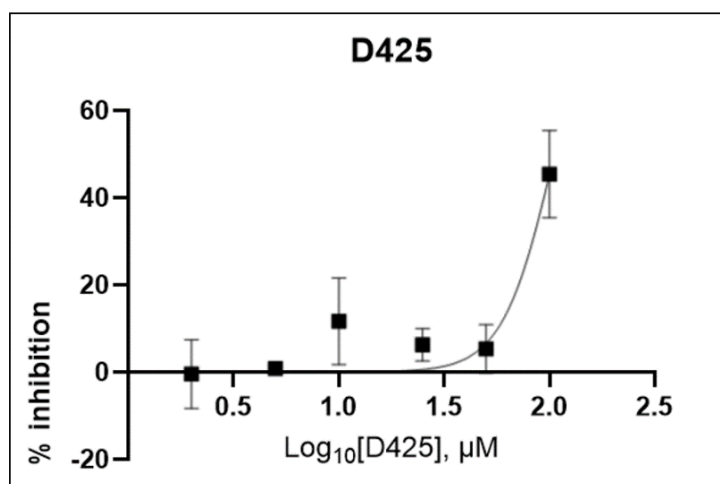


Figure 6. Dose-response curve for mPGES-1 enzyme inhibition of the compound **26**

Synthesis and antiproliferative activity of carvacrol-triazole conjugates

3.3. In Silico Studies

3.3.1. Molecular Docking and Conformation Analysis

In this study, we focused on evaluating *in silico* interactions of compound **26** with mPGES-1 and COX-1/2. MK-886 and co-crystallized ligands for each enzyme were used as reference compounds. All of these results are given in Table 4.

For mPGES-1 active site interactions, it is known that a potential inhibitor can act as a false substrate (PGH₂) and a cofactor analog (glutathione, GSH). Most of the known mPGES-1 inhibitors bind to the substrate and GSH binding sites simultaneously so that these compounds form U-shape conformation in the active site⁵⁵. *In silico* studies showed that compound **26** which is the best *in vitro* mPGES-1 enzyme inhibition, has two hydrogen bonds (GLU77, TYR130) between substituted sulfamoyl group and active site of related enzyme besides pi-cation interaction with the ARG126 residue.

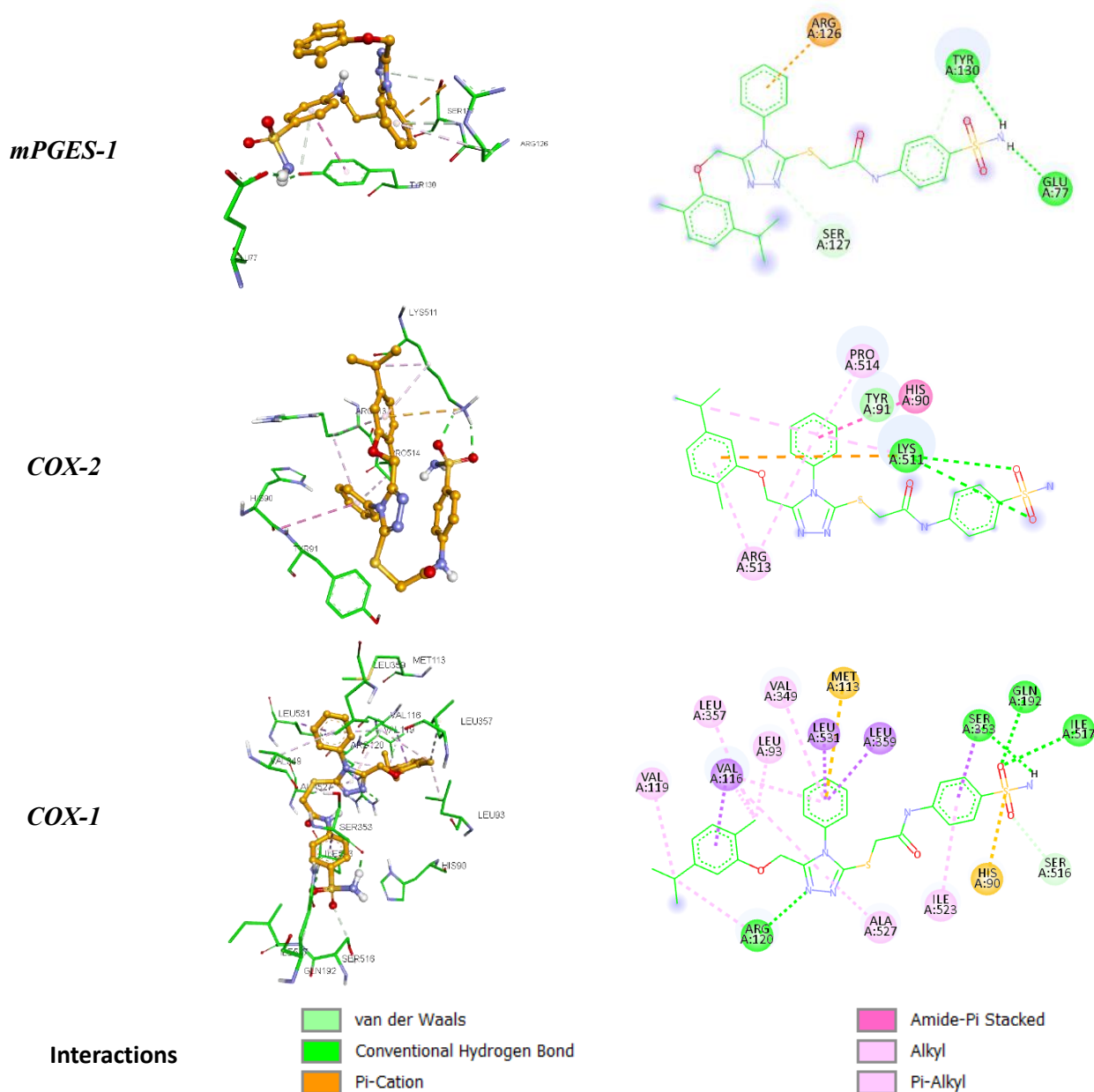


Figure 7. Active site interactions of compound **26** with mPGES-1, COX-1 and COX-2 as 3D and 2D diagrams

Additionally, compound **26** has exhibited strong binding site interactions for cyclooxygenase enzymes especially COX-1, too. The interactions of compound **26** with the active site of all three enzymes are given in the Figure 7

3.3.2. In Silico ADMET Studies

SMILES codes of the compounds **9-26** were generated from the ACD/ChemSketch version 12.0 molecular editor to determine their ADMET properties by using SwissADME calculation software (<http://www.swissadme.ch>). The number of hydrogen bond acceptors varied from 4 to 7 and number of rotatable bonds varied from 9 to 11, while any tested compounds have no more than 2 hydrogen bond donors (Table S1, see supplementary material). Estimated intestinal absorption (%ABS) of the synthesized compounds were calculated according to the method of Zhao *et al.* %ABS = $109 - [0.345 \times \text{topological polar surface area (TPSA)}]^{56}$ and determined between 52.81-76.45% ABS for all compounds. According to Lipinski's rule of five, molecular weight and LogP value should be smaller than 500 Da and 5, respectively. None of the compounds violated this Lipinski's rules except for compounds **18, 20, 22-26**. In addition to the any synthesized compounds were not exhibiting a mutagenic profile and no tumorigenic effect was observed except for compounds **12, 18** and **24**, too, according to the *in silico* toxicity predictions.

Table 4. Molecular docking results of compound **26**

Compound	Protein	Binding Energy (kcal/mol)	Number of H-bonds	Distance of H-bonds (Å)	H-bonding interactions	Hydrophobic interactions
26	mPGES-1 (5K0I)	-8.01	2	2.04	TYR130: H-N	ARG126 (pi-cation)
				1.80	GLU77: H-N	
				2.11	LYS511: O	HIS90 (amide-pi stacking)
	COX-2 (3NT1)	-8.01	2	2.13	LYS511: O	PRO514 (pi-pi stacking)
						ARG513 (pi-pi stacking)
				2.53	ARG120: N	VAL116 (pi-sigma)
	COX-1 (5WBE)	-8.10	4	1.77	SER353: H-N	LEU531 (pi-sigma)
				2.81	GLN192: O	LEU359 (pi-sigma)
				2.68	ILE517: O	
MK886	mPGES-1	-7.38				
	COX-2	-8.00				
	COX-1	-6.34				
Co-crystallized ligand	6PW (5K0I)	mPGES-1	-6.08			
	NPS (3NT1)	COX-2	-6.52			
	63X (5WBE)	COX-1	-9.56			

4. Conclusion

In conclusion, we present synthesis and characterization of a new series of carvacrol-containing 1,2,4-triazole derivatives **9-26** and evaluated their cytotoxic activity. The hybrid compounds were synthesized in adequate yields and purity as evidenced by HPLC analyses besides spectral characterization. *In vitro* anti-proliferative activities of the target molecules were evaluated by MTT assay against five cancer lines (human breast cancer MCF-7, human lung cancer A549, human prostate cancer PC-3, human chronic myelogenous leukemia K562, human neuroblastoma SH-SY5Y cell lines), as well as mouse embryonic fibroblast cells (NIH/3T3). The IC₅₀ value of the most active compound **26** was determined as 12.8 μ M using a cell viability assay (MTT assay) and xCELLigence real-time cell analysis. This compound induced apoptosis in a dose-dependent manner, by inducing caspase-9 signaling mechanism, also called the mitochondrial pathway. In addition, compound **26** significantly decreased the MMP in MCF-7 cells as an evidence for intrinsic pathway of apoptosis. Eighteen target compounds **9-26** were screened for their mPGES-1 and COX-1/2 inhibitory activities. Of these compounds, **26** showed the highest mPGES-1 inhibition at 10 μ M. As a result of *in silico* molecular modeling studies, it has been determined that compound **26** displays two hydrogen bonds and hydrophobic interactions with the active site of mPGES-1 in a U-shaped conformation. When the predicted toxicity profile of the compounds was examined, it was determined that compound **26**, which had the highest biological effect *in vitro*, had neither mutagenic nor tumorigenic effect.

Acknowledgments

This work was supported by The Scientific and Technological Research Council of Turkey (TÜBİTAK - Grant no. 218S549), European Union's Horizon 2020 research project ArthritisHeal under the Marie Skłodowska-Curie grant agreement (No. 812890).

Supporting Information

Supporting information accompanies this paper on <http://www.acgpubs.org/journal/organic-communications>

ORCID

İlker Demirbolat: [0000-0002-8756-1884](https://orcid.org/0000-0002-8756-1884)

Necla Kulabaş: [0000-0003-2273-5094](https://orcid.org/0000-0003-2273-5094)

Merve Gürboğa: [0000-0003-4614-7094](https://orcid.org/0000-0003-4614-7094)

Özlem Bingöl Özakpınar: [0000-0003-0287-5639](https://orcid.org/0000-0003-0287-5639)

Gamze Çiftçi: [0000-0001-7138-8012](https://orcid.org/0000-0001-7138-8012)

Kemal Yelekçi: [0000-0002-0052-4926](https://orcid.org/0000-0002-0052-4926)

Jiayang Liu: [0000-0002-8683-1109](https://orcid.org/0000-0002-8683-1109)

Per-Johan Jakobsson: [0000-0001-7665-9715](https://orcid.org/0000-0001-7665-9715)

Özkan Danış: [0000-0003-1781-0520](https://orcid.org/0000-0003-1781-0520)

Ayşe Ogan: [0000-0002-8973-9762](https://orcid.org/0000-0002-8973-9762)

İlkay Küçükgüzel: [0000-0002-7188-1859](https://orcid.org/0000-0002-7188-1859)

References

- [1] Kamel, M. M.; Megally Abdo, N. Y. Synthesis of novel 1,2,4-triazoles, triazolothiadiazines and triazolothiadiazoles as potential anticancer agents. *Eur. J. Med. Chem.* **2014**, *86*, 75–80.
- [2] Khazir, J.; Hyder, I.; Gayatri, J.; Prasad, L.; Nalla, N.; Chasoo, G.; Mahajan, A.; Saxena, A. K.; Alam, M. S.; Qazi, G. N.; Sampath, H. M. Design and synthesis of novel 1,2,3-triazole derivatives of coronopilin as anti-cancer compounds. *Eur. J. Med. Chem.* **2014**, *82*, 255–262.
- [3] Santucci, C.; Carioli, G.; Bertuccio, P.; Malvezzi, M.; Pastorino, U.; Boffetta, P.; Negri, E.; Bosetti, C.; La Vecchia, C. Progress in cancer mortality, incidence, and survival: a global overview. *Eur. J. Cancer Prev.* **2020**, *29* (5), 367–381.
- [4] Panathur, N.; Dalimba, U.; Venkat, P.; Alvala, M.; Yogeewari, P.; Sriram, D.; Kumar, V. Identification and characterization of novel indole based small molecules as anticancer agents through SIRT1 inhibition. *Eur. J. Med. Chem.* **2013**, *69*, 125–138.

- [5] Kulabaş, N.; Tatar, E.; Bingöl Özakpınar, Ö.; Özsavcı, D.; Pannecouque, C.; De Clercq, E.; Küçükgülzel, İ. Synthesis and antiproliferative evaluation of novel 2-(4H-1,2,4-triazole-3-Ylthio)acetamide derivatives as inducers of apoptosis in cancer cells. *Eur. J. Med. Chem.* **2016**, *121*, 58–70.
- [6] Ruan, D.; So, D. R. Prostaglandin E2 produced by inducible COX-2 and MPGES-1 promoting cancer cell proliferation in vitro and in vivo. *Life Sci.* **2014**, *116* (1), 43–50.
- [7] Bülbül, B.; Küçükgülzel, İ. Microsomal prostaglandin E2 synthase-1 as a new macromolecular drug target in the prevention of inflammation and cancer. *Anticancer. Agents Med. Chem.* **2019**, *19* (10), 1205–1222.
- [8] Sasaki, Y.; Nakatani, Y.; Hara, S. Role of microsomal prostaglandin E synthase-1 (MPGES-1)-derived prostaglandin E2 in colon carcinogenesis. *Prostaglandins Other Lipid Mediat.* **2015**, *121*, 42–45.
- [9] Chang, H. H.; Song, Z.; Wisner, L.; Tripp, T.; Gokhale, V.; Meuillet, E. J. Identification of a novel class of anti-inflammatory compounds with anti-tumor activity in colorectal and lung cancers. *Invest. New Drugs.* **2012**, *30*, 1865–1877.
- [10] Howe, L. R.; Subbaramaiah, K.; Kent, C. V.; Zhou, X. K.; Chang, S. H.; Hla, T.; Jakobsson, P. J.; Hudis, C. A.; Dannenberg, A. J. Genetic deletion of microsomal prostaglandin synthase-1 suppresses mouse mammary tumor growth and angiogenesis. *Prostaglandins Other Lipid Mediat.* **2013**, *106*, 99–105.
- [11] Hanaka, H.; Pawelzik, S. C.; Johnsen, J. I.; Rakonjac, M.; Terawaki, K.; Rasmuson, A.; Sveinbjörnsson, B.; Schumacher, M. C.; Hamberg, M.; Samuelsson, B.; Jakobsson, P. J.; Kogner, P.; Rådmark, O. Microsomal prostaglandin E synthase 1 determines tumor growth in vivo of prostate and lung cancer cells. *Proc. Natl. Acad. Sci.* **2009**, *106*, 18757–18762.
- [12] Van Rees, B. P.; Sivula, A.; Thorén, S.; Yokozaki, H.; Jakobsson, P. J.; Offerhaus, G. J. A.; Ristimäki, A. Expression of microsomal prostaglandin E synthase-1 in intestinal type gastric adenocarcinoma and in gastric cancer cell lines. *Int. J. Cancer* **2003**, *107*, 551–556.
- [13] Kock, A.; Larsson, K.; Bergqvist, F.; Eissler, N.; Elfman, L. H. M.; Raouf, J.; Korotkova, M.; Johnsen, J. I.; Jakobsson, P. J.; Kogner, P. Inhibition of microsomal prostaglandin E synthase-1 in cancer-associated fibroblasts suppresses neuroblastoma tumor growth. *eBioMedicine* **2018**, *32*, 84–92.
- [14] Jakobsson, P.-J.; Thoren, S.; Morgenstern, R.; Samuelsson, B. Identification of human prostaglandin E synthase: a microsomal, glutathione-dependent, inducible enzyme, constituting a potential novel drug target. *Proc. Natl. Acad. Sci.* **1999**, *96*, 7220–7225.
- [15] Finetti, F.; Terzuoli, E.; Bocci, E.; Coletta, I.; Polenzani, L.; Mangano, G.; Al-isi, M. A.; Cazzolla, N.; Giachetti, A.; Ziche, M.; Donnini, S. Pharmacological inhibition of microsomal prostaglandin E synthase-1 suppresses epidermal growth factor receptor-mediated tumor growth and angiogenesis. *PLoS One* **2012**, *7* (7), e40576.
- [16] Li, Y.; Yin, S.; Nie, D.; Xie, S.; Ma, L.; Wang, X.; Wu, Y.; Xiao, J. MK886 inhibits the proliferation of HL-60 leukemia cells by suppressing the expression of MPGES-1 and reducing prostaglandin E2 synthesis. *Int. J. Hematol.* **2011**, *94* (5), 42–478.
- [17] Bergqvist, F.; Ossipova, E.; Idborg, H.; Raouf, J.; Checa, A.; Englund, K.; Englund, P.; Khoonsari, P. E.; Kultima, K.; Wheelock, C. E.; Larsson, K.; Korotkova, M.; Jakobsson, P. J. Inhibition of MPGES-1 or COX-2 results in different proteomic and lipidomic profiles in A549 lung cancer cells. *Front. Pharmacol.* **2019**, *10* (June), 1–15.
- [18] Larsson, K.; Kock, A.; Idborg, H.; Arsenian Henriksson, M.; Martinsson, T.; Johnsen, J. I.; Korotkova, M.; Kogner, P.; Jakobsson, P.-J. COX/MPGES-1/PGE 2 pathway depicts an inflammatory-dependent high-risk neuroblastoma subset. *Proc. Natl. Acad. Sci.* **2015**, *112*, 8070–8075.
- [19] Nakanishi, M.; Rosenberg, D. W. Multifaceted roles of PGE2 in inflammation and cancer. *Semin. Immunopathol.* **2013**, *35*, 123–137.
- [20] Olesch, C.; Sha, W.; Angioni, C.; Sha, L. K.; Acaf, E.; Patrignani, P.; Jakobsson, P. J.; Radeke, H. H.; Grosch, S.; Geisslinger, G.; von Knethen, A.; Weigert, A.; Brune, B. MPGES-1-derived PGE2 suppresses CD80 expression on tumor-associated phagocytes to inhibit anti-tumor immune responses in breast cancer. *Oncotarget* **2015**, *6*, 10284–10296.
- [21] Nakanishi, M.; Menoret, A.; Tanaka, T.; Miyamoto, S.; Montrose, D. C.; Vella, A. T.; Rosenberg, D. W. Selective PGE(2) suppression inhibits colon carcinogenesis and modifies local mucosal immunity. *Cancer Prev. Res.* **2011**, *4*, 1198–1208.
- [22] Küçükgülzel, İ.; Küçükgülzel, S. G.; Rollas, S.; Kiraz, M. Some 3-thioxo/alkylthio-1,2,4-triazoles with a substituted thiourea moiety as possible antimycobacterials. *Bioorg. Med. Chem. Lett.* **2001**, *11* (13), 1703–1707.

Synthesis and antiproliferative activity of carvacrol-triazole conjugates

- [23] Küçükgülzel, S. G.; Küçükgülzel, I.; Tatar, E.; Rollas, S.; Sahin, F.; Güllüce, M.; De Clercq, E.; Kabasakal, L. Synthesis of some novel heterocyclic compounds derived from diflunisal hydrazide as potential anti-infective and anti-inflammatory agents. *Eur. J. Med. Chem.* **2007**, *42* (7), 893–901.
- [24] He, S.; Li, C.; Liu, Y.; Lai, L. Discovery of highly potent microsomal prostaglandin E2 synthase 1 inhibitors using the active conformation structural model and virtual screen. *J. Med. Chem.* **2013**, *56* (8), 3296–3309.
- [25] Erensoy, G.; Ding, K.; Zhan, C. G.; Çiftçi, G.; Yelekçi, K.; Duracık, M.; Bingöl Özakpınar, Ö.; Aydemir, E.; Yılmaz, Z. N.; Şahin, F.; Kulabaş, N.; Tatar, E.; Küçükgülzel, İ. Synthesis, in vitro and in silico studies on novel 3-Aayloxymethyl-5-[(2-oxo-2-arylethyl)sulfanyl]-1,2,4-triazoles and their oxime derivatives as potent inhibitors of MPGES-1. *J. Mol. Struct.* **2023**, *1272*, 134154.
- [26] Bülbül, B.; Ding, K.; Zhan, C. G.; Çiftçi, G.; Yelekçi, K.; Gürboğa, M.; Özakpınar, Ö. B.; Aydemir, E.; Baybağ, D.; Şahin, F.; Kulabaş, N.; Helvacıoğlu, S.; Charehsaz, M.; Tatar, E.; Özbey, S.; Küçükgülzel, İ. Novel 1,2,4-Triazoles derived from ibuprofen: synthesis and in vitro evaluation of their MPGES-1 inhibitory and antiproliferative activity. *Mol. Divers.* **2022**, (Early Access).
- [27] Al-Hussain, S. A.; Farghaly, T. A.; Zaki, M. E. A.; Abdulwahab, H. G.; Al-Qurashi, N. T.; Muhammad, Z. A. Discovery of novel indolyl-1,2,4-triazole hybrids as potent vascular endothelial growth factor receptor-2 (VEGFR-2) inhibitors with potential anti-renal cancer activity. *Bioorg. Chem.* **2020**, *105* (July), 104330.
- [28] Zengin, M.; Unsal Tan, O.; Arafa, R. K.; Balkan, A. Design and synthesis of new 2-oxoquinoxaliny-1,2,4-triazoles as antitumor VEGFR-2 inhibitors. *Bioorg. Chem.* **2022**, *121*, 105696.
- [29] Sharifi-Rad, M.; Varoni, E. M.; Iriti, M.; Martorell, M.; Setzer, W. N.; Del Mar Contreras, M. Salehi, B., Soltani-Nejad, A., Rajabi, S., Tajbakhsh, M., & Sharifi-Rad, J. Carvacrol and human health: a comprehensive review. *Phyther. Res.* **2018**, *32* (9), 1675–1687.
- [30] Kordali, S.; Cakir, A.; Ozer, H.; Ckamakcı, R.; Kesdek, M.; Mete, E. Antifungal, phytotoxic and insecticidal properteis of essential oil isolated turkish orifanum acutidens and its three components carvacrol, thymol and p-cymene. *Bioresour. Technol.* **2008**, *99*, 8788–8795.
- [31] Guarda, A.; Rubilar, J. F.; Miltz, J.; Galotto, M. J. The antimicrobial activity of microencapsulated thymol and carvacrol. *Int. J. Food Microbiol.* **2011**, *146*, 144–150.
- [32] Ghomi, J. S.; Ebrahimabadi, A. H.; Bidgoli, Z. D.; Batooli, H. GC/MS analysis and in vitro antioxidant activity of essential oil and methanol extracts of thymus caramicus jalas and its main constituent carvacrol. *Food Chem.* **2009**, *115*, 1524–1528.
- [33] Yin, Q. H.; Yan, F. X.; Zu, X. Y.; Wu, Y. H.; Wu, X. P.; Liao, M. C.; Deng, S. W.; Yin, L. I.; Zhuang, Y. Z. Anti-proliferative and pro-apoptotic effect of carvacrol on human hepatocellular carcinoma cell line HepG-2. *Cytotechnology* **2012**, *64*, 43–51.
- [34] Fan, K.; Xiaolei, L.; Cao, Y.; Qi, H.; Li, L.; Zhang, Q.; Sun, H. Carvacrol inhibits proliferation and induces apoptosis in human colon cancer cells. *Anticancer. Drugs* **2015**, *26* (8), 813–823.
- [35] Günes-Bayır, A.; Kızıltan, H. S.; Kocyigit, A.; Güler, E. M.; Karatas, E.; Toprak, A. Effects of natural phenolic compound carvacrol on the human gastric adenocarcinoma (AGS) cells in vitro. *Anticancer. Drugs* **2017**, *28*, 522–530.
- [36] Landa, P.; Kokoska, L.; Pribylova, M.; Vanek, T.; Marsik, P. In vitro anti-inflammatory activity of carvacrol: inhibitory effect on COX-2 catalyzed prostaglandin E2 biosynthesis. *Arch. Pharm. Res.* **2009**, *32*, 75–78.
- [37] Lima, M. D. S.; Quintans-Junior, L.; Santana, W. A. D.; Kaneto, C. M.; Soaers, M. B. P.; Villareal, C. F. Anti-inflammatory effects of carvacrol: evidence for a key role of interleukin-10. *Eur. J. Pharmacol.* **2013**, *699*, 112–117.
- [38] Khan, F.; Singh, V. K.; Saeed, M.; Kausar, M. A.; Ansari, I. A. Carvacrol Induced program cell death and cell cycle arrest in androgen-independent human prostate cancer cells via inhibition of notch signaling. *Anticancer. Agents Med. Chem.* **2019**, *19* (13), 1588–1608.
- [39] Li, L.; He, L.; Wu, Y.; Zhang, Y. Carvacrol affects breast cancer cells through TRPM7 mediated cell cycle regulation. *Life Sci.* **2021**, *266*, 118894.
- [40] Kulabaş, N.; Türe, A.; Bozdeveci, A.; Krishna, V. S.; Alpay Karaoğlu, Ş.; Sriram, D.; Küçükgülzel, İ. Novel fluoroquinolones containing 2-arylamino-2-oxoethyl fragment: design, synthesis, evaluation of antibacterial and antituberculosis activities and molecular modeling studies. *J. Heterocycl. Chem.* **2022**, *59* (5), 909–926.
- [41] Demirci, A.; Karayel, K. G.; Tatar, E.; Okullu, S. Ö.; Ünübol, N.; Taşlı, P. N.; Kocagöz, Z. T.; Sahin, F.; Küçükgülzel, İ. Synthesis and evaluation of novel 1,3,4-thiadiazole–fluoroquinolone hybrids as antibacterial, antituberculosis, and anticancer agents. *Turkish J. Chem.* **2018**, *42* (3), 839–858.

- [42] Şenkardaş, S.; Han, M. İ.; Kulabaş, N.; Abbak, M.; Çevik, Ö.; Küçükgülzel, İ.; Küçükgülzel, Ş. G. Synthesis, molecular docking and evaluation of novel sulfonyl hydrazones as anticancer agents and COX-2 inhibitors. *Mol. Divers.* **2020**, *24* (3), 673–689.
- [43] Larsson, K.; Steinmetz, J.; Bergqvist, F.; Arefin, S.; Spahiu, L.; Wannberg, J.; Pawelzik, S. C.; Morgenstern, R.; Stenberg, P.; Kublickiene, K.; Korotkova, M.; Jakobsson, P. J. Biological Characterization of new inhibitors of microsomal PGE synthase-1 in preclinical models of inflammation and vascular tone. *Br. J. Pharmacol.* **2019**, *176* (24), 4625–4638.
- [44] Kuklish, S. L.; Antonysamy, S.; Bhattachar, S. N.; Chandrasekhar, S.; Fisher, M. J.; Fretland, A. J.; Gooding, K.; Harvey, A.; Hughes, N. E.; Luz, J. G.; Manninen, P. R.; McGee, J. E.; Navarro, A.; Norman, B. H.; Partridge, K. M.; Quimby, S. J.; Schiffler, M. A.; Sloan, A. V.; Warshawsky, A. M.; York, J. S.; Yu, X. P. Characterization of 3,3-dimethyl substituted n-aryl piperidines as potent microsomal prostaglandin E synthase-1 inhibitors. *Bioorganic Med. Chem. Lett.* **2016**, *26* (19), 4824–4828.
- [45] Cingolani, G.; Panella, A.; Perrone, M. G.; Vitale, P.; Di Mauro, G.; Fortuna, C. G.; Armen, R. S.; Ferorelli, S.; Smith, W. L.; Scilimati, A. Structural basis for selective inhibition of cyclooxygenase-1 (COX-1) by diarylisoxazoles mofezolac and 3-(5-chlorofuran-2-yl)-5-methyl-4-phenylisoxazole (P6). *Eur. J. Med. Chem.* **2017**, *138*, 661–668.
- [46] Duggan, K. C.; Walters, M. J.; Musee, J.; Harp, J. M.; Kiefer, J. R.; Oates, J. A.; Marnett, L. J. Molecular basis for cyclooxygenase inhibition by the non-steroidal anti-inflammatory drug naproxen. *J. Biol. Chem.* **2010**, *285* (45), 34950–34959.
- [47] Morris, G. M.; Huey, R.; Lindstrom, W.; Sanner, M. F.; Belew, R. K.; Goodsell, D. S.; Olson, A. J. Software news and updates gabedit — a graphical user interface for computational chemistry softwares. *J. Comput. Chem.* **2009**, *30* (16), 174–182.
- [48] Morris, G. M.; Goodsell, D. S.; Halliday, R. S.; Huey, R.; Hart, W. E.; Belew, R. K.; Olson, A. J. Automated docking using a lamarckian genetic algorithm and an empirical binding free energy function. *J. Comput. Chem.* **1998**, *19* (14), 1639–1662.
- [49] Daina, A.; Michielin, O.; Zoete, V. SwissADME: A free web tool to evaluate pharmacokinetics, drug-likeness and medicinal chemistry friendliness of small molecules. *Sci. Rep.* **2017**, *7*, 1–13.
- [50] Sander, T.; Freyss, J.; Von Korff, M.; Rufener, C. DataWarrior: An open-source program for chemistry aware data visualization and analysis. *J. Chem. Inf. Model.* **2015**, *55* (2), 460–473.
- [51] Tatar, E.; Küçükgülzel, G.; Karakuş, S.; de Clercq, E.; Andrei, G.; Snoeck, R.; Pannecouque, C.; Öktem Okullu, S.; Ünübol, N.; Kocagöz, T.; Kalayci, S.; ŞahİN, F.; Küçükgülzel, İ. Synthesis and biological evaluation of some new 1,3,4-thiadiazole and 1,2,4-triazole derivatives from l-methionine as antituberculosis and antiviral agents. *Marmara Pharm. J.* **2015**, *19* (2), 88–102.
- [52] Othman, E. M.; Fayed, E. A.; Husseiny, E. M.; Abulhair, H. S. Apoptosis induction, PARP-1 Inhibition, and cell cycle analysis of leukemia cancer cells treated with novel synthetic 1,2,3-triazole-chalcone conjugates. *Bioorg. Chem.* **2022**, *123*, 105762.
- [53] Othman, E. M.; Fayed, E. A.; Husseiny, E. M.; Abulhair, H. S. The effect of novel synthetic semicarbazone- and thiosemicarbazone-linked 1,2,3-triazoles on the apoptotic markers, VEGFR-2, and cell cycle of myeloid leukemia. *Bioorg. Chem.* **2022**, *127*, 105968.
- [54] Özsvacı, D.; Erşahin, M.; Şener, A.; Bingöl Özakpınar, Ö.; Zorlu Toklu, H.; Akakın, D.; Şener, G.; Yeğen, B. Ç. The novel function of Nesfatin-1 as an anti-inflammatory and antiapoptotic peptide in subarachnoid hemorrhage-induced oxidative brain damage in rats. *Neurosurgery* **2011**, *68*, 1699–1708.
- [55] Khurana, P.; Jachak, S. M. Chemistry and biology of microsomal prostaglandin E2 synthase-1 (MPGES-1) Inhibitors as novel anti-inflammatory agents: recent developments and current status. *RSC Adv.* **2016**, *6* (34), 28343–28369.
- [56] Zhao, Y. H.; Abraham, M. H.; Le, J.; Hersey, A.; Luscombe, C. N.; Beck, G.; Sherborne, B.; Cooper, I. Rate-limited steps of human oral absorption and QSAR studies. *Pharm. Res.* **2002**, *19* (10), 1446–1457.